

Potent antitumor effect of tumor microenvironment-targeted oncolytic adenovirus against desmoplastic pancreatic cancer

Yan Li¹, JinWoo Hong², Joung-Eun Oh², A-Rum Yoon² and Chae-Ok Yun ²

¹ Graduate Program for Nanomedical Science, Yonsei University, Seoul, Korea

² Department of Bioengineering, College of Engineering, Hanyang University, Seongdong-Gu, Seoul, Korea

Pancreatic cancer is a leading cause of cancer-related death. Desmoplastic pancreatic tumors exhibit excessive extracellular matrix (ECM) and are thus highly resistant to anticancer therapeutics, since the ECM restricts drug penetration and dispersion. Here, we designed and generated two hypoxia-responsive and cancer-specific hybrid promoters, H(mT)E and H(E)mT. Transgene expression driven by each hybrid promoter was markedly higher under hypoxic conditions than normoxic conditions. Moreover, H(E)mT-driven transgene expression was highly cancer-specific and was superior to that of H(mT)E-driven expression. A decorin-expressing oncolytic adenovirus (Ad; oH(E)mT-DCN) replicating under the control of the H(E)mT promoter induced more potent and highly cancer-specific cell death compared with its cognate control oncolytic Ad, which harbored the endogenous Ad E1A promoter. Moreover, oH(E)mT-DCN exhibited enhanced antitumor efficacy compared with both the clinically approved oncolytic Ad ONYX-015 and its cognate control oncolytic Ad lacking DCN. oH(E)mT-DCN treatment also attenuated the expression of major ECM components, such as collagen I/III, elastin and fibronectin and induced tumor cell apoptosis, leading to extensive viral dispersion within orthotopic pancreatic tumors and pancreatic cancer patient-derived tumor spheroids. Collectively, these findings demonstrate that oH(E)mT-DCN exhibits potent antitumor efficacy by degrading the ECM and inducing apoptosis in a multifunctional process. This process facilitates the dispersion and replication of oncolytic Ad, making it an attractive candidate for the treatment of aggressive and desmoplastic pancreatic cancer.

Pancreatic cancer is the fourth leading cause of cancer-related death in Europe and the United States.¹ Only 10–20% of all patients with pancreatic cancer are resectable at presentation. The US National Cancer Institute recently reported that the overall 5-year relative survival rate for 2002–2008 was 5.8%, and nearly 90% of all patients were dead 1 year after diagnosis, with a median survival of <6 months.^{2,3} One experimental treatment option of particular interest for pancreatic cancer is oncolytic virotherapy, which uses viral vectors to preferentially replicate in tumor cells and induce cancer cell death. Among the various viral vectors that have been tested, adenovirus (Ad) has been most extensively used

in gene therapy applications, and sufficient data from randomized clinical trials support its safety in patients.^{4–6} Although oncolytic Ad-mediated cancer gene therapy is highly promising, significant therapeutic efficacy of oncolytic Ad for the treatment of localized tumors has not yet been achieved in clinical trials; thus, further improvements are needed.^{7,8}

Hypoperfusion and desmoplasia are two prominent features of pancreatic cancer that attenuate the therapeutic efficacy of cancer therapeutics.⁹ Aberrant extracellular matrix (ECM) functions as a protective layer that prevents drug penetration and diffusion into the pancreatic tumors, contributing to poor disease management by conventional treatment modalities. Furthermore, hypoxia, a condition characterized by oxygen deprivation caused by abnormal microcirculation and vascularization in the tumor microenvironment, promotes cancer progression and attenuates the therapeutic efficacy of oncolytic Ad by suppressing viral replication through downregulation of Ad E1A protein expression.^{10–12}

Decorin (DCN), a ubiquitous component of the ECM, is preferentially found in association with collagen fibrils. Furthermore, DCN regulates the production of other ECM components by blocking the activity of transforming growth factor- β (TGF- β), which is a major inducer of desmoplasia in pancreatic tumors.¹³ We previously demonstrated that oncolytic Ad-mediated intratumoral expression of DCN can drive degradation of the ECM and inhibit ECM production, thereby enhancing viral penetration and dispersion within

Key words: oncolytic adenovirus, pancreatic cancer, decorin, hypoxia, desmoplasia, cancer-specific promoter, extracellular matrix
Additional Supporting Information may be found in the online version of this article.

Conflicts of Interest: No potential conflicts of interest were disclosed.

Grant sponsor: The research fund of Hanyang University; **Grant number:** HY-2011-G-20110000001880

DOI: 10.1002/ijc.31060

History: Received 13 Jan 2017; Accepted 5 Sep 2017; Online 20 Sep 2017

Correspondence to: Dr. Chae-Ok Yun, Ph.D. Department of Bioengineering, College of Engineering, Hanyang University, 222 Wangsimni-ro, Seongdong-gu, Seoul, Korea, Tel.: [82-2-2220-0491], Fax: +[82-2-2220-4850], E-mail: chaeok@hanyang.ac.kr

What's new?

We have generated a novel hypoxia-responsive and cancer-specific hybrid promoters (oH(E)mT) to drive the replication of decorin (DCN)-expressing oncolytic Ad (oH(E)mT-DCN) to overcome multiple microenvironmental barriers in desmoplastic pancreatic tumor. oH(E)mT-DCN showed extensive viral distribution in patient-derived pancreatic tumor spheroids and orthotopic pancreatic tumor through effective degradation of aberrant extracellular matrix and hypoxia-responsiveness of oH(E)mT promoter. To best of our knowledge, this is the first report illustrating that DCN expression mediated by hypoxia-responsive and cancer-specific hybrid promoters-driven oncolytic Ad can overcome several critical hurdles proposed by the tumor microenvironment of desmoplastic pancreatic tumors.

solid tumors and making DCN a promising therapeutic gene for the treatment of desmoplastic tumors.¹⁴

A successful oncolytic Ad-mediated cancer gene therapy requires good cancer-specificity, since ectopic replication of Ad at nontarget tissues will result in cytotoxicity. In this regard, numerous studies have been conducted with the aim of achieving selective replication of Ad in a cancer cell-specific manner. A particularly promising approach for endowing cancer-specificity to replication-competent Ad is to restrict viral replication to cancer cells by replacing the endogenous Ad promoter with a cancer cell-specific promoter. Among the cancer-specific promoters, both the E2F and human telomerase reverse transcriptase (hTERT) promoters have demonstrated good cancer specificity.^{15,16} We previously showed that oncolytic Ad replicating under the control of a modified hTERT (mTERT) promoter containing additional c-Myc and Sp1 binding sites replicates more efficiently and preferentially in tumor cells than its cognate control Ad replicating under the wild-type hTERT promoter, resulting in more potent Ad E1A-mediated apoptosis and viral cytolysis in a cancer-restricted manner.¹⁷ However, the therapeutic effect of oncolytic Ad in the hypoxic region of the tumor nest was still insufficient, since hypoxia directly impacts the therapeutic efficacy of oncolytic Ad by suppressing viral replication through attenuation of Ad E1A protein expression.^{10–12}

To overcome this hypoxia-induced downregulation of Ad E1A expression in solid tumors and to enhance their cancer-selective promoter activity, we designed and generated two different enhancer/promoter hybrids that incorporate 6 copies of the hypoxia response element (HRE) upstream of either the E2F or mTERT promoter. This strategy generated an HRE-mTERT-E2F hybrid promoter (H(mT)E) and an HRE-E2F-mTERT hybrid promoter (H(E)mT). In this study, we demonstrate that DCN-expressing oncolytic Ad replicating under the control of the H(E)mT hybrid promoter (oH(E)mT-DCN) exerts potent tumoricidal effects by efficaciously and preferentially replicating in both hypoxic and normoxic regions of highly desmoplastic pancreatic tumors.

Material and Methods**Cell lines and cell culture**

All cell lines with the exception of normal pancreatic cells (NPC), which was maintained in prigrrow I medium, were cultured in Dulbecco's modified Eagle's medium (GIBCO

BRL, Grand Island, NY) supplemented with 10% fetal bovine serum (GIBCO BRL) and penicillin-streptomycin (100 IU/mL, GIBCO BRL). The HEK293 (human embryonic kidney cell line expressing the Ad E1 region), A549 (human lung cancer cell line), MIA PaCa-2 and PANC-1 (pancreatic cancer cell lines) and human dermal fibroblast (HDF; normal fibroblast cell line) cell lines were purchased from the American Type Culture Collection (Manassas, VA). The NPC cell line was purchased from Applied Biological Materials (ABM, Richmond, Canada). All cell lines were maintained at 37°C in a humidified atmosphere at 5% CO₂.

Animal studies

Six to eight-week-old male athymic nude mice were purchased from Charles River Korea (Seongnam, South Korea) and maintained in a laminar air flow cabinet under specific pathogen-free environment. All facilities were approved by AAALAC (Association for Assessment and Accreditation of Laboratory Animal Care). All of the animal experiments were conducted according to the institutional guidelines established for the Hanyang University Institutional Animal Care and Use Committee.

Construction of the Ad vectors

To generate the two different cancer-specific hybrid promoters, HRE/mTERT/E2F (H(mT)E) and HRE/E2F/mTERT (H(E)mT), the HRE enhancer, E2F and the mTERT promoter were inserted into pdE1sp1B, thereby generating pdE1sp1B-H(mT)E and pdE1sp1B-H(E)mT.^{10,17,18} To construct E1 shuttle vectors expressing green fluorescent protein (GFP) under the control of the modified cancer-specific promoters (H(mT)E and H(E)mT), the sequence encoding GFP was subcloned from pEGFP-N1 using *Xho* I/*Afl* II. This GFP gene was then ligated into pdE1sp1B/H(mT)E and pdE1sp1B/H(E)mT cut with the same restriction enzymes, thereby generating the pdE1sp1B/H(mT)E-GFP and pdE1sp1B/H(E)mT-GFP Ad E1 shuttle vectors. The Ad E1 shuttle vectors were linearized by *Xmn* I digestion, whereas the Ad vector dE1-k35 was linearized with *Bst*B I digestion. The linearized Ad shuttle vectors were cotransformed into *Escherichia coli* BJ5183 cells with *Bst*B I-digested dE1-k35 to allow for homologous recombination. The resultant homologously recombined Ad plasmid was digested with *Pac* I and transfected into HEK293 cells to generate the replication-

incompetent Ads, dH(mT)E-GFP and dH(E)mT-GFP (Supporting Information Fig. S1A). GFP-expressing Ad under the control of the cytomegalovirus (CMV) promoter (dCMV-GFP) was used as a control.^{19,20}

To create an oncolytic Ad replicating under the control of the H(E)mT promoter, a template Ad plasmid consisting of the E1B 19 kDa region-deleted E1 shuttle vector (pdE1sp1B/Rd19) harboring the retinoblastoma binding sites of mutant E1A was used.^{21,22} Initially, the H(E)mT promoter was inserted into pdE1sp1B/Rd19, thereby generating the pdE1sp1B/H(E)mT-Rd19 Ad E1 shuttle vector. To create a DCN-expressing replicating Ad vector, the sequence encoding DCN was subcloned from pCA14/DCN using *Bgl* II into pdE1sp1B/H(E)mT-Rd19, thereby generating the pdE1sp1B/H(E)mT-Rd19/DCN Ad E1 shuttle vector. These Ad E1 shuttle vectors (pdE1sp1B/Rd19, pdE1sp1B/H(E)mT-Rd19, and pdE1sp1B/H(E)mT-Rd19/DCN) were linearized with *Xmn* I and then cotransformed into *Escherichia coli* BJ5183 cells with linearized dE1-k35 to allow for homologous recombination, thus generating the oRd19 (Rd19-k35), oH(E)mT (H(E)mT-Rd19-k35) and oH(E)mT-DCN (H(E)mT-Rd19-k35/DCN) oncolytic Ad plasmids, respectively. The resultant homologously recombined Ad plasmids were digested with *Pac* I and transfected into HEK293 cells to generate the replication-competent Ads oRd19, oH(E)mT and oH(E)mT-DCN (Supporting Information Fig. S1B).

Replication-incompetent Ad and replication-competent oncolytic Ad were propagated in HEK293 cells and A549 cells, respectively. All viruses were obtained as previously described.²¹ The numbers of viral particles (VP) were calculated from optical density measurements at 260 nm (OD_{260}), where 1 absorbency unit ($OD_{260} = 1$) indicated a concentration of 1.1×10^{12} VP/mL. Purified viruses were stored at -80°C until use.

Transduction efficiency analysis

To assess the transcriptional activity of the H(mT)E and H(E)mT promoters under normoxic and hypoxic conditions, fluorescence microscopy and fluorescence-activated cell sorting (FACS) analysis were carried out. Pancreatic cancer cells (MIA PaCa-2 and PANC-1) were transduced with GFP-expressing replication-incompetent Ad under the control of the H(mT)E or the H(E)mT promoter at a multiplicity of infection (MOI) of 50. At 48 hr post-transduction, cells were imaged using a fluorescence microscope (Carl Zeiss, Thornwood, NY), and the GFP expression levels were quantified using a FACSCalibur analyzer (Becton-Dickinson, San Jose, CA). All FACS data were analyzed using CellQuest software (Becton-Dickinson). Approximately 10,000 events were counted for each sample.

To assess the cancer specificity of the CMV and H(E)mT promoters, fluorescence microscopy and FACS analysis were carried out. Cells were transduced with GFP-expressing Ad under the control of the CMV promoter or the H(E)mT promoter at MOIs of 5, 20 and 50. At 48 hr post-transduction,

cells were imaged by fluorescence microscopy, and the GFP expression level was quantified using a FACSCalibur analyzer and CellQuest software. Approximately 10,000 events were counted for each sample.

MTT assay

To evaluate the extent to which H(E)mT-regulated oncolytic Ad (oH(E)mT) selectively kills cancer cells, pancreatic cancer cells (MIA PaCa-2 and PANC-1) and normal cells (NPCs and HDFs) seeded in 24-well plates were infected with oH(E)mT (or oRd19 as the cognate control) at an MOI of 2 under either normoxic or hypoxic conditions. At 60 hr post-infection, 200 μL of 3-(4,5-dimethylthiazol-2-yl)-2,5-diphenyl-tetrazolium bromide (MTT; Sigma, St. Louis, MO) in phosphate-buffered saline (PBS; 2 mg/mL) was added to each well. After 4 hr of incubation at 37°C , the supernatant was discarded from each well, and the precipitate was dissolved in dimethylsulfoxide. The absorbance of each well at 540 nm was then read on a microplate reader. All assays were performed in triplicate. The number of living cells in the untreated cell group was analyzed in an identical manner as a negative control.

To evaluate the extent to which DCN-expressing oncolytic Ad (oH(E)mT-DCN) and the control oncolytic Ad (oH(E)mT) specifically kill cancer cells, and to determine whether this effect is dose-dependent, pancreatic cancer cells (MIA PaCa-2 and PANC-1) and normal cells (NPCs and HDFs) were grown in 24-well plates to 50–60% confluency. Next, cells were infected with oH(E)mT or oH(E)mT-DCN at an MOI of 1, 2 or 5. At 72 hr postinfection, the MTT assay was performed as described above.

In addition, the kinetics of pancreatic cancer cell killing by oncolytic Ads (oH(E)mT and oH(E)mT-DCN) was analyzed by the MTT assay. Specifically, upon reaching ~50–60% confluence, cells in 24-well plates were infected (MOI = 2) with oH(E)mT or oH(E)mT-DCN. The MTT assay was then performed at 24, 48 and 72 hr post-infection as described above.

Virus production assay

To assess the viral production of oncolytic Ads, pancreatic cancer cells and normal cells were seeded in 24-well plates at ~60% confluency and then infected with oRd19 or oH(E)mT at an MOI of 0.5 (pancreatic cancer cells) or 10 (normal cells). After 48 hr of incubation at 37°C under either normoxic or hypoxic conditions, supernatants and cell pellets were collected and freeze-thawed three times to release internal virus. Real-time quantitative PCR (Q-PCR; TaqMan PCR detection; Applied Biosystems, Foster City, CA) was used to assess the number of viral genomes in each sample. Samples were analyzed in triplicate, and data were processed using the SDS 19.1 software package (Applied Biosystems).

Enzyme-linked immunosorbent assay (ELISA) measuring the levels of secreted DCN and TGF- β 1 expression

Pancreatic cancer cells (MIA PaCa-2 and PANC-1) and normal cells (NPCs and HDFs) were seeded in 24-well plates at ~60% confluency and then infected with oH(E)mT-DCN at an MOI of 0.5 or 2. At 2 days post-infection, supernatants were collected by centrifugation at 15,000 *g* for 10 min at 4°C, and the level of secreted DCN was assessed using an ELISA kit (Abcam, Cambridge, UK).

To evaluate TGF- β 1 expression in tumor tissue, tumor tissues were collected from mice treated with PBS or oncolytic Ads (ONYX-015, oH(E)mT or oH(E)mT-DCN) at 30 days after the administration of the first viral treatment. Tumor tissues were homogenized in ice-cold RIPA buffer (Elipis Biotech, Taejeon, South Korea) containing a proteinase inhibitor cocktail (Sigma). Homogenates were then centrifuged in a high-speed microcentrifuge for 10 min, after which total protein contents were determined using a BCA protein assay kit (Pierce, Rockford, IL). The level of TGF- β 1 was measured by a conventional ELISA kit (R&D Systems, Minneapolis, MN).

Assessment of antitumor effects in an orthotopic model of human pancreatic cancer

MIA PaCa-2 cells (5×10^6), which stably express firefly luciferase, were injected into the pancreas of athymic nude mice. At 2 weeks post-implantation (Day 0), mice were divided into four separate groups in order to receive intraperitoneal treatment of PBS, ONYX-015, oH(E)mT or oH(E)mT-DCN ($n = 6$ per group). Optical imaging was carried out every five days following the first treatment with an IVIS Spectrum instrument (Xenogen Corp., Alameda, CA). Image signals were quantitatively analyzed with IGOR-PRO Living Image software (Xenogen). At 30 days after the first treatment, tumors were collected, imaged, weighed and sectioned.

Western blot analysis

To evaluate the levels of DCN and Ad E1A protein expression in tumor cell lysates from MIA PaCa-2 pancreatic orthotopic models, tumors were collected from Ad-treated mice at 30 days after the first viral treatment. Similarly, the cells were infected with ONYX-015 (2 MOI), oH(E)mT (2 MOI) or oH(E)mT/DCN (0.5 or 2 MOI) for 48 hr and then cells were harvested to analyze intracellular expression level of DCN and apoptosis-related proteins by western blotting. Both cell lysates and tumors were homogenized in ice-cold RIPA buffer containing a proteinase inhibitor cocktail. The resultant homogenates were then centrifuged in a high-speed microcentrifuge for 10 min. Protein concentrations were determined by the BCA protein assay, and equal protein amounts were resolved by sodium dodecyl sulfate-polyacrylamide gel electrophoresis. The proteins were electrotransferred to polyvinylidene fluoride membranes and incubated with goat anti-DCN antibodies (Ab; R&D Systems),

rabbit anti-Ad E1A (Santa Cruz Biotechnology, Santa Cruz, CA), rabbit anti-cleaved caspase-3 (Cell Signaling Technology, Beverly, MA), rabbit anti-poly (ADP-ribose) polymerase (PARP) (Cell Signaling Technology) or rabbit anti- β -actin Abs (Cell Signaling Technology). Next, the membranes were incubated with secondary horseradish peroxidase-conjugated goat anti-rabbit IgG or mouse anti-goat IgG Abs (Cell Signaling). Immunoreactive bands were visualized *via* enhanced chemiluminescence (Amersham Pharmacia Biotech, Uppsala, Sweden). The expression levels of Ad E1A and DCN were semiquantitatively analyzed using ImageJ software (National Institutes of Health, Bethesda, MD).

Histology and immunohistochemistry

Representative sections were stained with hematoxylin and eosin (H & E), picosirius red or Masson's trichrome (Sigma) and then examined using a light microscope (Carl Zeiss). Pancreatic tumor tissue sections and pancreatic tumor spheroid sections were incubated at 4°C overnight with mouse anti-collagen type I (Abcam), mouse anti-collagen type III (Sigma), mouse anti-elastin (Sigma), mouse anti-fibronectin (Santa Cruz Biotechnology), rabbit anti-Ad E1A or mouse anti-proliferating cell nuclear antigen (PCNA; DAKO, Glostrup, Denmark) primary Abs and then treated with an ABC-peroxidase kit (ChemMate DAKO Envision kit; DAKO, Carpinteria, CA). All slides were counterstained with Meyer's hematoxylin (Sigma), with the exception of picosirius red-stained and Masson's trichrome-stained slides, which were counterstained with Harris' hematoxylin (Sigma). Collagen expression was detected by Masson's trichrome or picosirius red staining, whereas the expression levels of Ad E1A, PCNA, type I and III collagen, elastin and fibronectin in tumor tissues were detected by specific antibody staining. Expression levels were semiquantitatively analyzed using MetaMorph® image analysis software (Universal Image, Buckinghamshire, UK). Each result is expressed as the mean optical density of five different digital images.

Immunofluorescence staining

For immunofluorescence staining of Ad E1A and hypoxia-inducible factor 1 α (HIF-1 α), tumor sections were treated with rabbit anti-Ad E1A Ab or mouse anti-human HIF-1 α Abs (Abcam) and incubated overnight at 4°C. Next, the tumor sections were treated with Alexa Fluor 568 (red)-conjugated goat anti-rabbit IgG (Invitrogen, Carlsbad, CA) or Alexa Fluor 488 (green)-conjugated goat anti-mouse IgG (Invitrogen) Abs at room temperature for 1 hr. For counterstaining, the samples were incubated with 4,6-diamidino-2-phenylindole (Sigma). The slides were mounted with Vectashield mounting medium (Vector Laboratories, Burlingame, CA) and imaged under a confocal laser-scanning microscope (LSM510, Carl Zeiss MicroImaging, Thornwood, NY).

Terminal deoxynucleotidyl transferase dUTP nick end labeling assay

Formalin-fixed and paraffin-embedded tissue sections (5- μ m) were deparaffinized and rehydrated according to standard protocols.²³ Apoptosis was detected terminal deoxynucleotidyl transferase dUTP nick end labeling (TUNEL) assay (DeadEnd™ Fluorometric TUNEL System; Promega, Madison, WI). Briefly, tissue sections were permeabilized with proteinase K (20 mg/mL) for 10 min at room temperature. Sections were then incubated with terminal deoxynucleotidyl transferase (TdT) and fluorescein-12-dUTP in TdT buffer at room temperature for 60 min and washed with TdT buffer. Finally, nuclei were counterstained with methyl green (Sigma). The samples were analyzed by light microscopy. The amount of apoptotic cells was semiquantitatively analyzed using MetaMorph® image analysis software. Each result is expressed as the mean optical density of five different digital images.

Preparation of pancreatic cancer patient-derived tumor spheroids

Primary pancreatic cancer tumors were obtained from patients with active-stage pancreatic cancer ($n = 3$). Pancreatic cancer patient-derived tumor spheroids were prepared as previously described.¹⁴ Plates containing the tumor spheroids were treated with oncolytic Ad (1×10^{10} VP of ONYX-015, oH(E)mT, or oH(E)mT-DCN) on days 1 and 4 and incubated at 37°C for 6 days. The treated tumor spheroids were then fixed with 10% formalin, embedded in paraffin and cut into 5- μ m-thick sections.

Statistical analysis

All data are expressed as mean \pm standard deviation (SD). Statistical significance was determined by the two-tailed Student's *t* test (SPSS 13.0 software; SPSS, Chicago, IL) and one-way ANOVA. Differences were considered statistically significant at $*p < 0.05$, $**p < 0.01$ and $***p < 0.001$.

Results

Potent and tumor-selective activity of the H(E)mT promoter

The E2F and TERT promoters are established cancer-specific promoters that have been frequently utilized to endow cancer specificity to Ads.^{15,17} However, cancer-specific promoters alone cannot prevent the attenuation of Ad replication in the context of the hypoxic tumor microenvironment. To overcome hypoxia-induced downregulation of Ad E1A expression and enhance the promoter activity in cancer cells, we constructed two variants of a cancer-specific hybrid promoter, HRE/E2F/mTERT (H(E)mT) and HRE/mTERT/E2F (H(mT)E), by inserting six copies of the HRE upstream of either the E2F or mTERT promoter.

To compare the promoter activities of the HRE-harboring hybrid promoters, two different replication-incompetent Ads expressing GFP under the control of the H(E)mT or H(mT)E

promoter were generated (dH(mT)E-GFP and dH(E)mT-GFP, respectively; Supporting Information Fig. S1A). Pancreatic cancer cells (MIA PaCa-2 and PANC-1) were then transduced with either dH(mT)E-GFP or dH(E)mT-GFP, which were under the control of the hybrid promoters, for 48 hr. As shown in Figures 1a and 1b, dH(E)mT-GFP induced significantly higher GFP expression than dH(mT)E-GFP under normoxic conditions in both MIA PaCa-2 and PANC-1 cells ($**p < 0.01$, $***p < 0.001$, respectively), demonstrating the superior transcriptional activity of the H(E)mT promoter. More importantly, H(E)mT promoter activity was significantly enhanced under hypoxic conditions compared with normoxic conditions ($***p < 0.001$), demonstrating that insertion of the HRE enhancer upstream of a cancer-specific hybrid promoter can enhance Ad-mediated transgene expression under hypoxic conditions. Similar trends were observed in cancer cells of different tissue origins (Supporting Information Fig. S2A). Based on these results, the H(E)mT promoter was selected as a more potent promoter than the H(mT)E promoter and was utilized in subsequent experiments.

To assess the cancer selectivity of the H(E)mT promoter, pancreatic cancer cells (MIA PaCa-2 and PANC-1) or normal cells (NPCs and HDFs) were transduced with replication-incompetent GFP-expressing Ad under the control of either the CMV or H(E)mT promoter (dCMV-GFP and dH(E)mT-GFP, respectively). As shown in Figures 1c and 1d, both dCMV-GFP and dH(E)mT-GFP conferred a dose-dependent increase in relative GFP expression in pancreatic cancer cells. In contrast, negligible GFP expression was observed in dH(E)mT-GFP-transduced normal cells (Fig. 1c and Supporting Information S2B), even at a high MOI of 50. In contrast, dCMV-GFP induced dose-dependent GFP expression in normal cells. Of particular note, dH(E)mT-GFP induced 31.9-fold and 72.0-fold lower GFP expression than dCMV-GFP at an MOI of 50 in NPC and HDF cells, respectively ($***p < 0.001$). These results demonstrate that the H(E)mT promoter is highly cancer cell-selective, exhibits good transcriptional activity in tumor cells and drives only minimal transcriptional activity in normal cells.

Cancer cell-specific killing effect of H(E)mT promoter-regulated oncolytic Ad

We previously reported that oncolytic Ad containing mutated E1A retinoblastoma binding sites and harboring a deletion of the E1B 19 kDa region (oRd19) exhibits potent cancer cell killing efficacy and good cancer specificity.^{21,24} In an effort to improve the cancer cell-specific viral replication and killing effects, we replaced the endogenous oRd19 promoter of the Ad E1A gene with the H(E)mT promoter, thus generating an oH(E)mT oncolytic Ad (Supporting Information Fig. S1B).

To assess whether oH(E)mT oncolytic Ad could replicate and induce cell killing in a cancer-selective manner, cancer and normal cells were infected with oRd19 or oH(E)mT for 60 hr at an MOI of 2. As shown in Figure 2, oH(E)mT killed

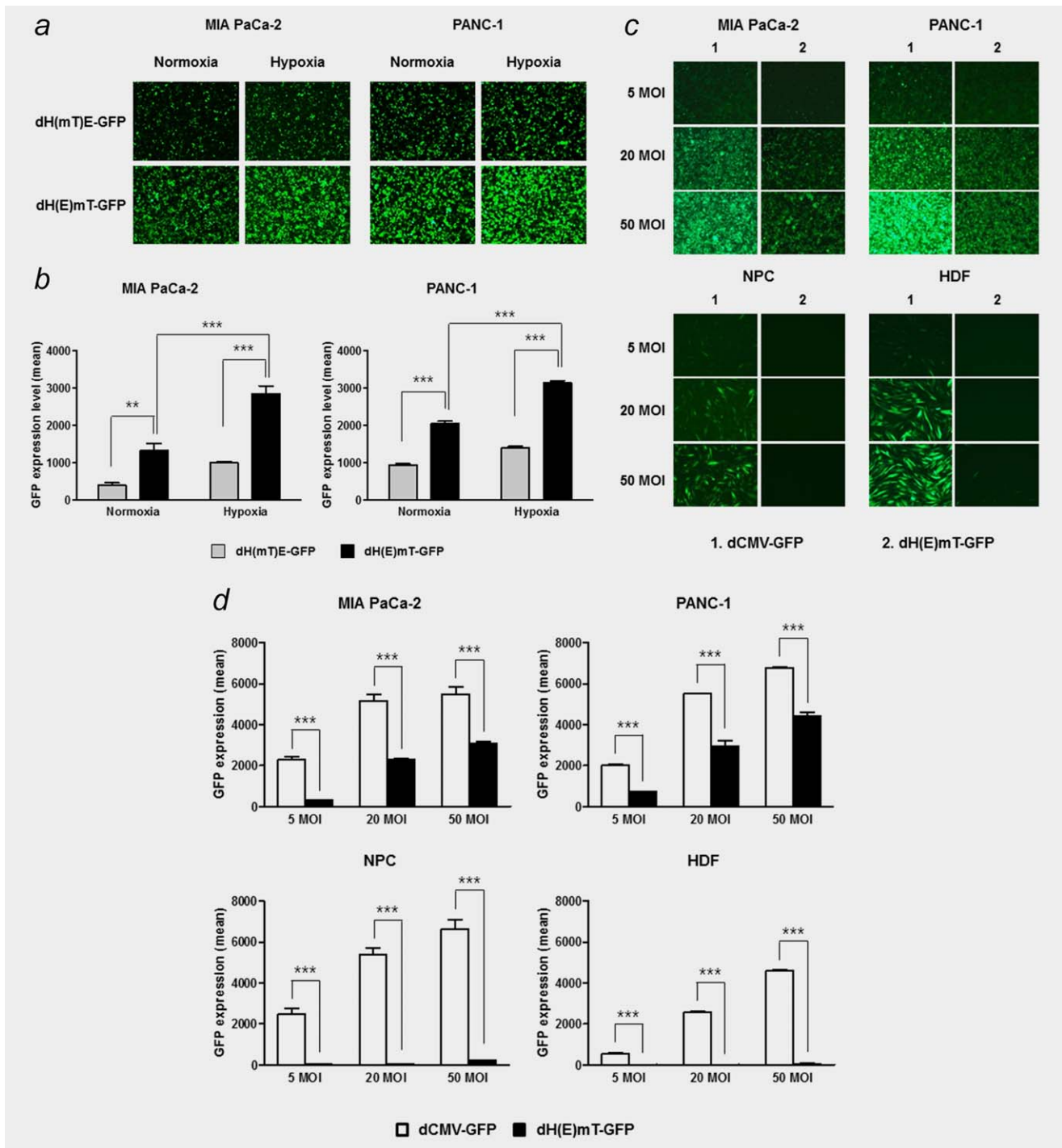


Figure 1. GFP expression driven by the cancer cell-specific promoter. (a, b) Levels of GFP expression driven by the H(mT)E or H(E)mT promoter in human pancreatic cancer cell lines (MIA PaCa-2 and PANC-1). Cells were transduced with Ads expressing GFP under the control of the H(mT)E or H(E)mT promoter (dH(mT)E or dH(E)mT) at an MOI of 50 under normoxic or hypoxic conditions. (c, d) Levels of GFP expression driven by the CMV or H(E)mT promoter (dCMV or dH(E)mT) in human pancreatic cancer (MIA PaCa-2 and PANC-1) and normal cell lines (NPC and HDF). Cells were transduced with Ads expressing GFP under the control of the CMV or H(E)mT promoter at an MOI of 5, 20 or 50. Fluorescence images (a and b) and quantitative FACS analysis (c and d) of GFP expression. Expression was analyzed after 48 hr incubation at 37°C. Data shown are representative of three independent experiments, each performed in triplicate. Bars represent mean ± SD. ***p* < 0.01 and ****p* < 0.001. [Color figure can be viewed at wileyonlinelibrary.com]

pancreatic cancer cells (MIA PaCa-2 and PANC-1) more efficiently than oRd19 under both normoxic and hypoxic conditions (***p* < 0.001), whereas no cell killing was observed in

normal cells (NPCs and HDFs). These findings indicate that oH(E)mT exhibits more potent cancer cell-specific killing efficacy than oRd19. Of particular note, oH(E)mT was not

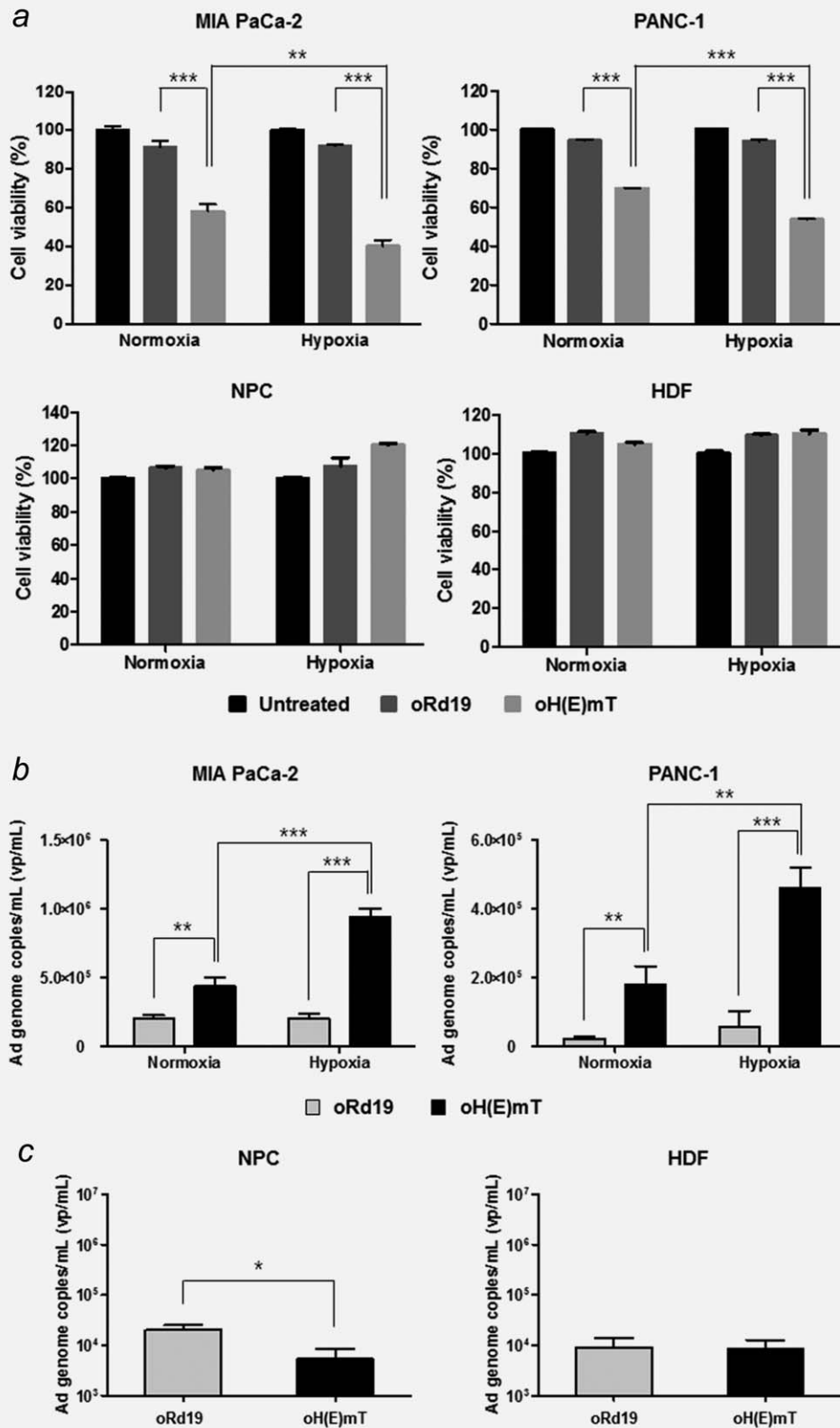


Figure 2. Cancer cell killing efficacy of oRd19 and oH(E)mT under normoxic and hypoxic conditions (a). Pancreatic cancer and normal cells were treated with oRd19 or oH(E)mT at an MOI of 2. Cell viability was assessed by the MTT assay. The viability of untreated cells was set to 100%. Data shown are representative of three independent experiments, each performed in triplicate. Bars represent mean \pm SD.

** $p < 0.01$ and *** $p < 0.001$. Viral production of oRd19 and oH(E)mT (b and c). Cells were treated with oRd19 or oH(E)mT at an MOI of 0.5 (pancreatic cancer cells) or 10 (normal cells). Viral production was assessed by Q-PCR at 48 hr after infection. Data shown are representative of three independent experiments, each performed in triplicate. Bars represent mean \pm SD. * $p < 0.05$, ** $p < 0.01$ and *** $p < 0.001$.

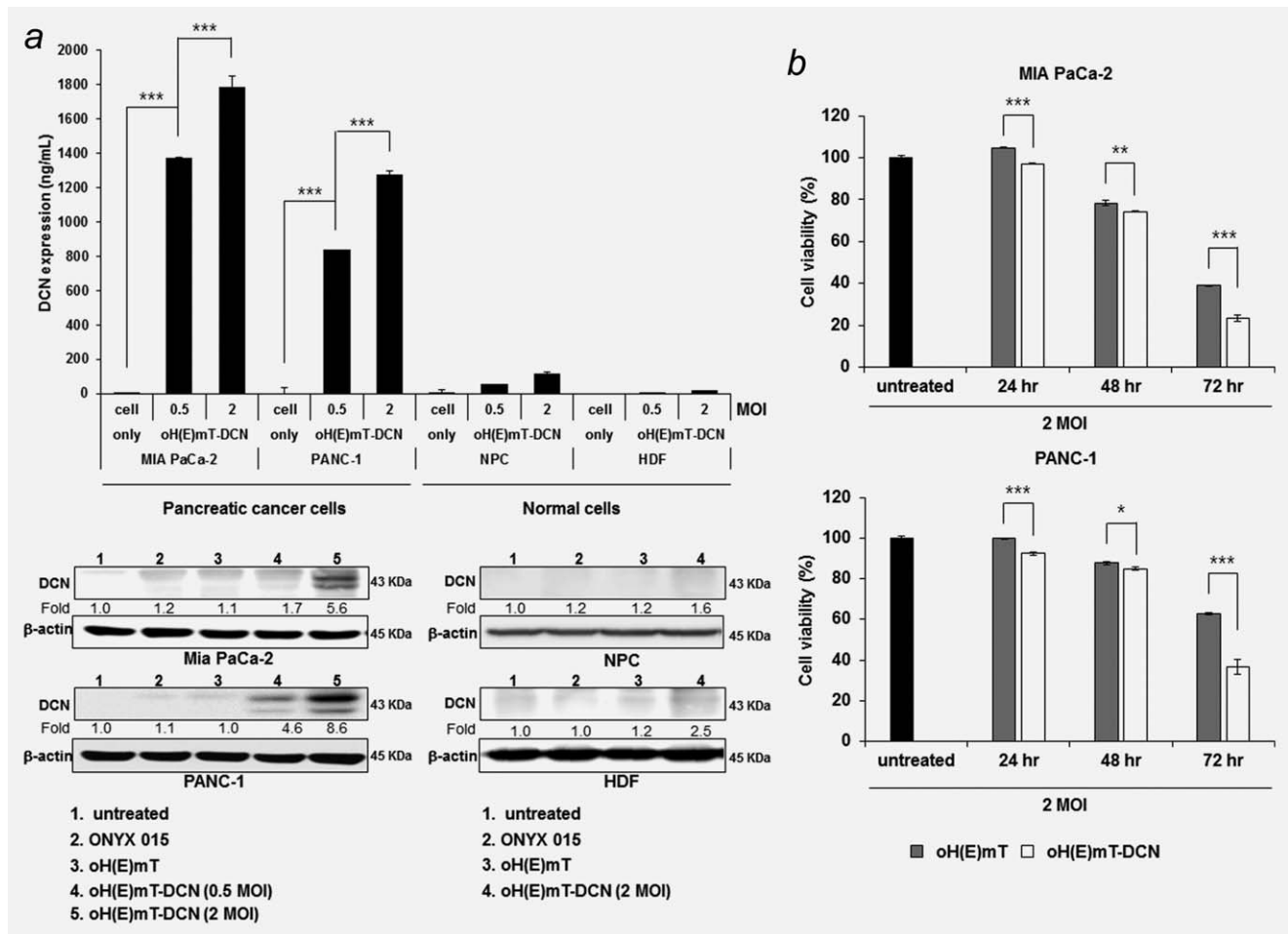


Figure 3. DCN expression in pancreatic cancer and normal cells infected with oH(E)mT-DCN (a). Cells were treated with oH(E)mT-DCN at an MOI of 0.5 or 2. DCN expression was assessed at 48 hr after infection by DCN ELISA. Similarly, these cells were treated with ONYX-015, oH(E)mT or oH(E)mT-DCN and intracellular DCN expression level was detected from cell lysates at 48 hr post treatment. Data shown are representative of three independent experiments, each performed in triplicate. Bars represent mean ± SD. ****p* < 0.001. Cancer cell killing efficacy of oH(E)mT and oH(E)mT-DCN. Pancreatic cancer and normal cells were treated with oH(E)mT or oH(E)mT-DCN. The MTT assay was carried out at various time points (b) or after treatment with various MOIs (c). The viability of untreated cells was set to 100%. Data shown are representative of three independent experiments, each performed in triplicate. Bars represent mean ± SD. **p* < 0.05, ***p* < 0.01 and ****p* < 0.001.

cytotoxic to normal cells under hypoxic conditions, indicating that incorporation of the HRE enhancer into the oH(E)mT promoter did not affect the cancer specificity of oncolytic Ad under hypoxic conditions. Specifically, oH(E)mT exhibited significantly higher cancer cell killing under hypoxic conditions than under normoxic conditions (18.1% and 16.0% higher than in normoxic conditions in MIA PaCa-2 and PANC-1 cells, respectively; ***p* < 0.01, ****p* < 0.001). In contrast, no significant difference was detected in pancreatic cancer cells treated with oRd19 under hypoxic vs. normoxic conditions, indicating that oH(E)mT can overcome hypoxia-mediated attenuation of Ad E1A protein expression.

Cancer cell-restricted replication of Ads controlled by the H(E)mT promoter

To assess whether oH(E)mT-induced cytotoxicity was dependent on viral replication, pancreatic cancer cells were infected for 48 hr at an MOI of 0.5 with oH(E)mT or its cognate

control, oRd19 (Figs. 2b and 2c). In MIA PaCa-2 cells, oH(E)mT exhibited 2.1-fold and 4.6-fold higher viral production than oRd19 under normoxic and hypoxic conditions, respectively (***p* < 0.01, ****p* < 0.001). Similar results were observed in PANC-1 cells. These results indicate that the activity of the H(E)mT promoter is superior in both normoxic and hypoxic conditions to that of the endogenous Ad E1A promoter. Furthermore, viral replication of oH(E)mT was significantly lower than, or similar to, that of oRd19 in NPCs and HDFs at a high MOI (10), indicating that H(E)mT promoter-driven viral replication is highly cancer-specific.

Cancer cell-specific expression of DCN by oH(E)mT-DCN

Desmoplasia, a prominent pathological attribute of pancreatic cancer, is marked by a dramatic increase in the proliferation of fibroblasts and increased deposition of ECM components.²⁵ Aberrant deposition of ECM components affects the

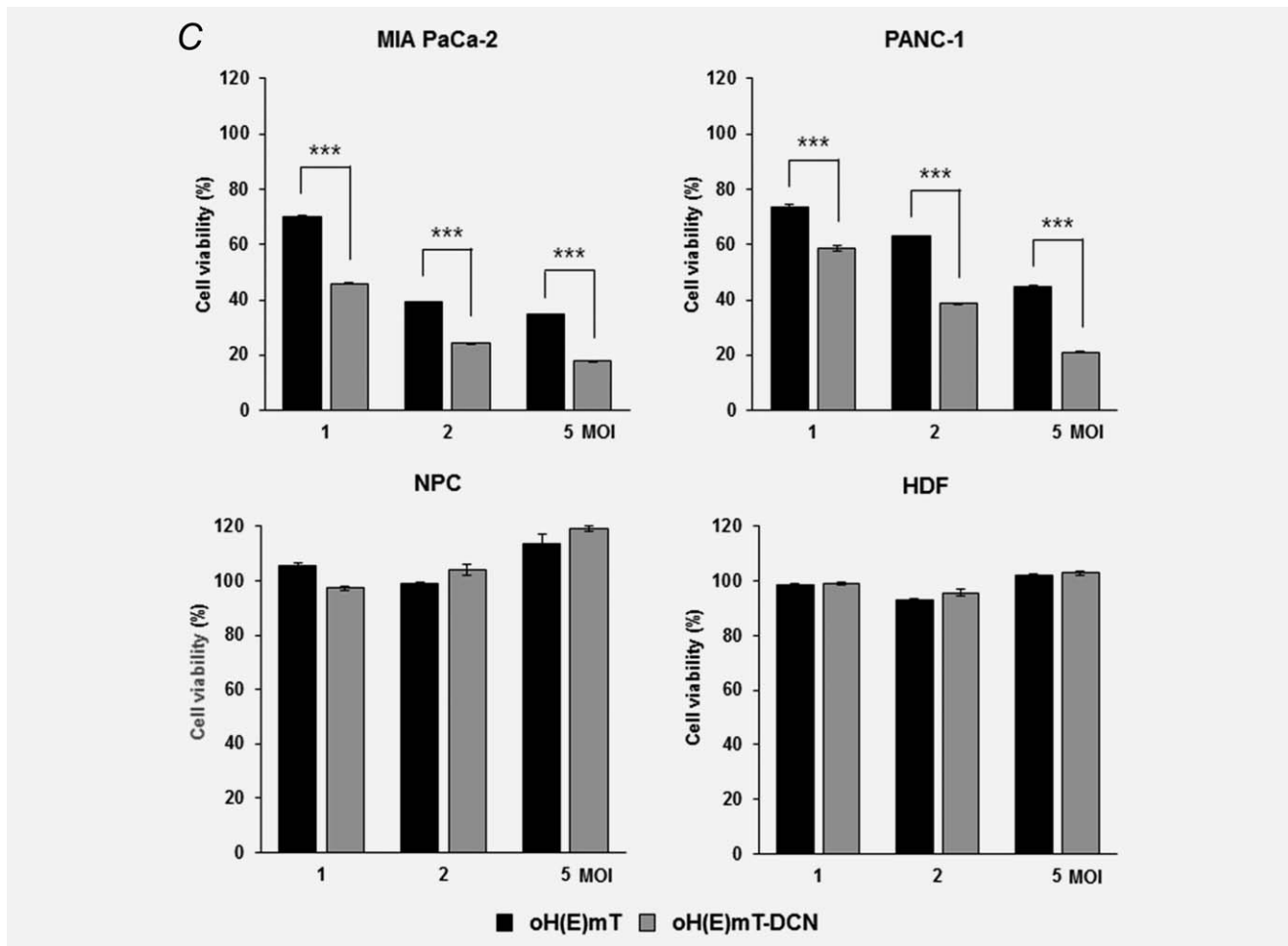


Figure 3. Continued.

overall elasticity and interstitial fluid pressure of the tumor, which can contribute to chemoresistance and poor viral distribution.^{14,25} To maximize the therapeutic efficacy of oncolytic Ad for the treatment of pancreatic tumors, we generated an H(E)mT promoter-driven oncolytic Ad expressing DCN (oH(E)mT-DCN). Our rationale for generating this Ad was that DCN can degrade aberrant ECM components such as collagen, elastin and fibronectin (Supporting Information Fig. S1B).

To assess whether oH(E)mT-DCN could induce cancer cell-specific expression of DCN, pancreatic cancer and normal cells were infected with oH(E)mT-DCN at an MOI of 0.5 or 2 and culture supernatants were examined for DCN secretion by ELISA and intracellular DCN expression was detected from cell lysates by western blotting. As shown in Figure 3a dose-dependent increase in DCN expression was observed in pancreatic cancer cells infected with oH(E)mT-DCN ($***p < 0.001$). In marked contrast, only negligible DCN expression was detected in normal cells. Taken together, these results indicate that oH(E)mT-DCN can efficiently express DCN in a cancer cell-restricted manner,

presumably due to the H(E)mT promoter-mediated cancer-specific replication of oncolytic Ad.

Enhanced cancer cell-specific killing of DCN-expressing oncolytic Ad

We have previously reported that DCN-expressing Ad shows increased viral dissemination and greater cytotoxicity than control Ad by inducing apoptosis.¹⁴ To determine whether oH(E)mT-DCN can more efficiently induce killing of pancreatic cancer cells than oH(E)mT, an MTT assay was performed to assess cell viability at various time points (Fig. 3b) and after infection with different MOIs (Fig. 3c). Both oH(E)mT and oH(E)mT-DCN elicited a time-dependent increase in pancreatic cancer cell killing efficacy, indicating that both oncolytic Ads replicate efficiently and induce cancer cell death. Importantly, oH(E)mT-DCN was significantly more cytotoxic to cancer cells than oH(E)mT at all time points ($*p < 0.05$, $**p < 0.01$, $***p < 0.001$). Furthermore, the magnitude of difference in cancer cell killing efficacy was greater at later time points, suggesting that replication of

oH(E)mT-DCN and subsequent amplification of DCN expression contributed to the potent cytopathic effect.

As shown in Figure 3c, both oH(E)mT and oH(E)mT-DCN exhibited dose-dependent cytotoxicity to pancreatic cancer cells. Importantly, oH(E)mT-DCN was significantly more cytotoxic to cancer cells than oH(E)mT at all doses in MIA PaCa-2 and PANC-1 cells, further implying that oncolytic Ad-mediated expression of DCN enhances the potency of oncolytic Ad ($***p < 0.001$). Furthermore, both oncolytic Ads induced only negligible cell death in normal cells, indicating that DCN expression is not detrimental to normal cells and that DCN-mediated cell killing is cancer-selective. Additionally, both oH(E)mT and oH(E)mT-DCN showed cancer-specific and dose-dependent increase in viral replication, suggesting oH(E)mT promoter driven cytolytic effect will occur preferentially in cancer cells (Supporting Information Fig. S3). This result is consistent with a previous report in which DCN-mediated induction of apoptosis was shown to be cancer-specific.¹⁴ Altogether, these results demonstrate that DCN expression mediated by oH(E)mT-DCN enhances the dose-dependent and time-dependent cytotoxicity of oncolytic Ad, which occurs specifically in cancer cells.

Therapeutic efficacy of oH(E)mT and oH(E)mT-DCN in orthotopic pancreatic cancer

Orthotopic tumor models are emerging as a prominent model of cancer progression; moreover, the microenvironment of orthotopic tumors closely emulates that of clinical tumors.^{26,27} To evaluate the therapeutic potential of oH(E)mT-DCN against pancreatic cancer, we assessed the extent to which oncolytic Ads (oH(E)mT or oH(E)mT-DCN) could inhibit tumor growth in an orthotopic pancreatic cancer model. As a control, we used ONYX-015, a clinically approved oncolytic Ad. To monitor and visualize the growth of the orthotopic tumors in real time, orthotopic pancreatic tumors were established by injecting firefly luciferase-expressing MIA PaCa-2 pancreatic cancer cells into the pancreas of Balb/c nude mice. Tumor growth was then monitored by bioluminescence optical imaging.

As shown in Figures 4a and 4b, the orthotopic pancreatic tumors continued to grow for up to 30 days after the initial treatment in PBS-treated, ONYX-015-treated, or oH(E)mT-treated mice. In contrast, oH(E)mT-DCN treatment resulted in a markedly lower tumor growth rate ($***p < 0.001$ vs. PBS; $**p < 0.01$ vs. ONYX-015, oH(E)mT). At 30 days after the initial treatment, the increase in total flux of PBS-treated, ONYX-015-treated, oH(E)mT-treated and oH(E)mT-DCN-treated mice averaged 22.2, 24.9, 14.7 and 1.4-fold higher than the initial measurement, respectively. Surprisingly, ONYX-015 (which is clinically approved) did not suppress tumor growth, suggesting that the highly aggressive nature of orthotopic pancreatic tumors renders them refractory to treatment with ONYX-015. In marked contrast, both oH(E)mT and oH(E)mT-DCN suppressed tumor growth more effectively than ONYX-015, implying that H(E)mT

promoter-driven oncolytic Ads are highly effective for the treatment of pancreatic tumors. Importantly, oH(E)mT-DCN inhibited tumor growth to a greater extent than oH(E)mT, suggesting that oncolytic Ad-mediated DCN expression enhances the antitumor efficacy of oncolytic Ad ($*p < 0.05$, $***p < 0.001$). Similarly, tumor weight measurements indicated that oH(E)mT-DCN was a more potent inhibitor of tumor growth than ONYX-015 or oH(E)mT (Fig. 4c; $***p < 0.001$ versus ONYX-015 and $*p < 0.05$ vs. oH(E)mT), further supporting our conclusion that oHEmT-DCN is well-suited for the treatment of aggressive pancreatic tumors.

To further investigate the mechanisms behind the antitumor effects of the different oncolytic Ads, Western blotting was performed to analyze the levels of Ad E1A and DCN expression in the tumors. As shown in Figure 5a, oH(E)mT and oH(E)mT-DCN induced markedly higher expression of Ad E1A in tumor tissue than ONYX-015, implying that the H(E)mT promoter induces high levels of viral replication in pancreatic tumors. Importantly, oH(E)mT-DCN induced 2.1-fold and 4.1-fold higher expression of Ad E1A and DCN, respectively, compared with oH(E)mT.

The TGF- β signaling pathway plays a critical role in the disease progression of cancer. This pathway regulates cell growth, differentiation, migration and induces the epithelial-to-mesenchymal transition.²⁸ DCN has been reported to suppress the biological activity of TGF- β by preventing TGF- β binding to its receptor.^{14,29} Therefore, we performed ELISA to assess whether DCN expression mediated by oncolytic Ads affects the intratumoral expression level of TGF- β . As shown in Figure 5b, the intratumoral expression level of TGF- β was significantly suppressed (by 32.6% and 26.8%) following treatment with oH(E)mT-DCN compared with the PBS and oH(E)mT treatments, respectively ($**p < 0.01$, $***p < 0.001$). In contrast, no reduction of TGF- β expression was observed in ONYX-015-treated tumor tissue. Together, these results demonstrate that DCN expression is positively correlated with the suppression of TGF- β expression, and the potent antitumor efficacy of oH(E)mT-DCN was mediated by efficient viral replication, DCN expression and subsequent downregulation of TGF- β .

Histologic, TUNEL and immunohistochemical characterization

The antitumor efficacy of the intraperitoneally administered oncolytic Ads was further investigated by histological and immunohistochemical analyses. H & E staining revealed a marked reduction in the number of viable tumor cells and more extensive necrotic regions in oH(E)mT-treated and oH(E)mT-DCN-treated tumors compared with PBS-treated and ONYX-015-treated tumors (Fig. 5c). Importantly, most of the oH(E)mT-DCN-treated tumor tissue was necrotic, whereas necrotic lesions were detected only in the central region of the oH(E)mT-treated tumor tissue, indicating that oH(E)mT-DCN can disperse through tumor tissue more effectively than oH(E)mT. Moreover, no necrosis was

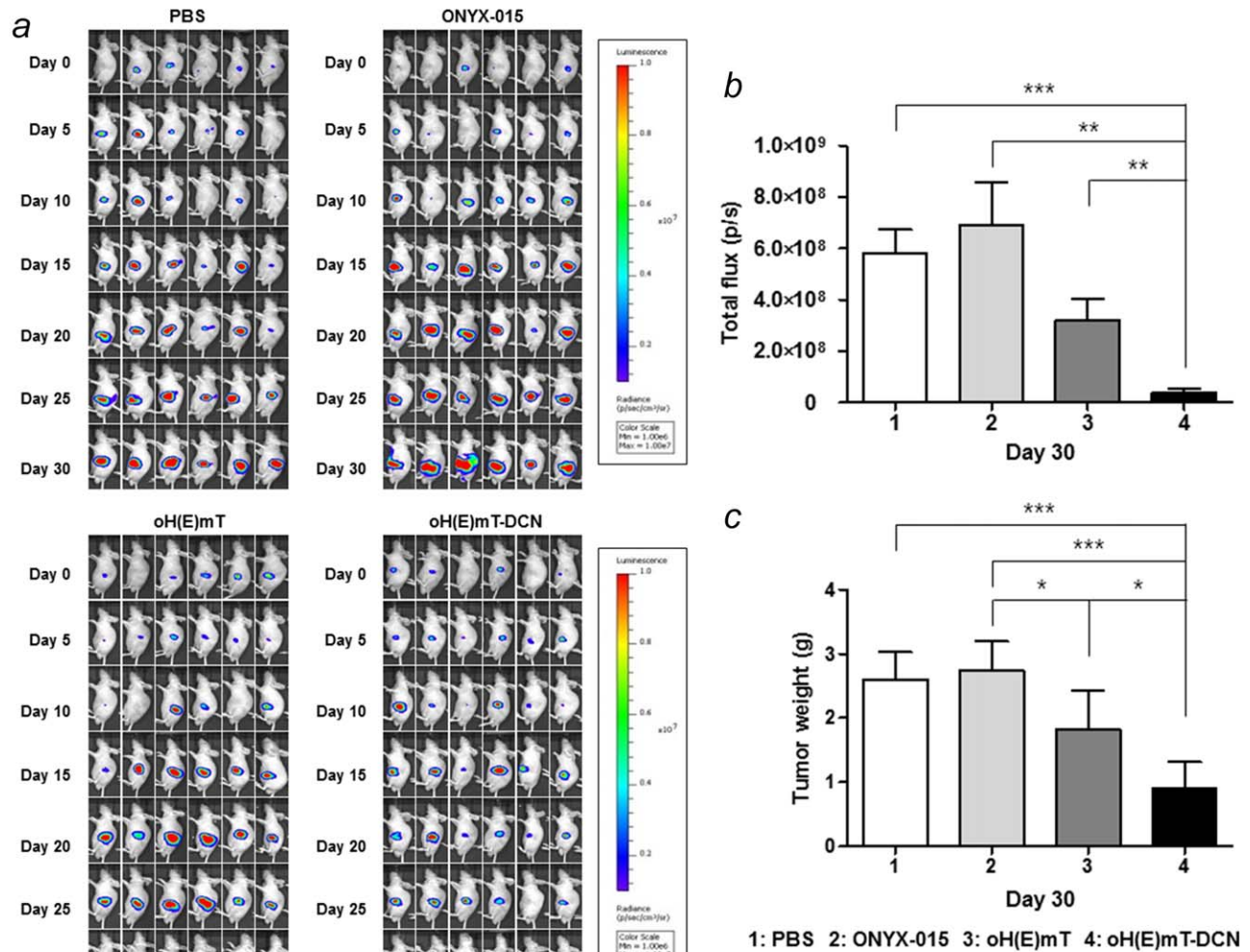


Figure 4. Potent tumor growth inhibition by DCN-expressing oncolytic Ad in a pancreatic orthotopic tumor xenograft model. (a) Nude mice with MIA PaCa-2 orthotopic pancreatic tumors were intraperitoneally injected with PBS, ONYX-015, oH(E)mT or oH(E)mT-DCN at two-day intervals. Firefly luciferase expression was monitored every 5 days after treatments using an IVIS imaging system. (b) Bioluminescence signals were calculated in total flux of photons/sec (p/sec) after background subtraction from the region of interest. (c) Tumors were harvested at 30 days following the first treatment and measured. Plots were generated of the tumor weights. Then, tumor tissues were lysed to generate total protein extracts. [Color figure can be viewed at wileyonlinelibrary.com]

observed in normal tissues adjacent to the oH(E)mT-DCN-treated tumor tissues, suggesting that oH(E)mT-DCN preferentially induces necrosis in tumors.

Ad E1A staining revealed that the oH(E)mT-DCN-treated tumors exhibited markedly higher accumulation of Ad, through a greater area of the tumor, than ONYX-015-treated or oH(E)mT-treated tumors, indicating that expression of DCN facilitates viral replication and spreading within solid tumors. Consistent with the H & E staining results, no Ad E1A staining was observed in the surrounding normal tissues. This finding further confirms that the therapeutic effect of oH(E)mT-DCN is highly cancer-specific, and that tumor cell necrosis is induced by efficient viral replication-mediated cytolysis.

Tumor cell proliferation was markedly attenuated in oH(E)mT-DCN-treated tumors, as assessed by PCNA

staining. Furthermore, a markedly higher percentage of tumor cells was undergoing apoptosis in oH(E)mT-DCN-treated tumors compared with PBS-treated, ONYX-015-treated, or oH(E)mT-treated tumors, as assessed by the TUNEL assay. In line with these results, we observed that oH(E)mT-DCN induced dose-dependent expression of proapoptotic signaling molecules, such as cleaved caspase 3 and PARP, in comparison to oH(E)mT *in vitro* (Supporting Information Fig. S4), confirming that DCN induces apoptosis of cancer cells.

Hypoxia, a hallmark of the tumor microenvironment, has been reported to attenuate replication of oncolytic Ad,¹⁰ leading to insufficient therapeutic efficacy in hypovascular regions of solid tumors. Therefore, we examined the extent of replication of oncolytic Ads in hypoxic tumor regions. As shown in Figure 5d, high levels of oH(E)mT and oH(E)mT-DCN

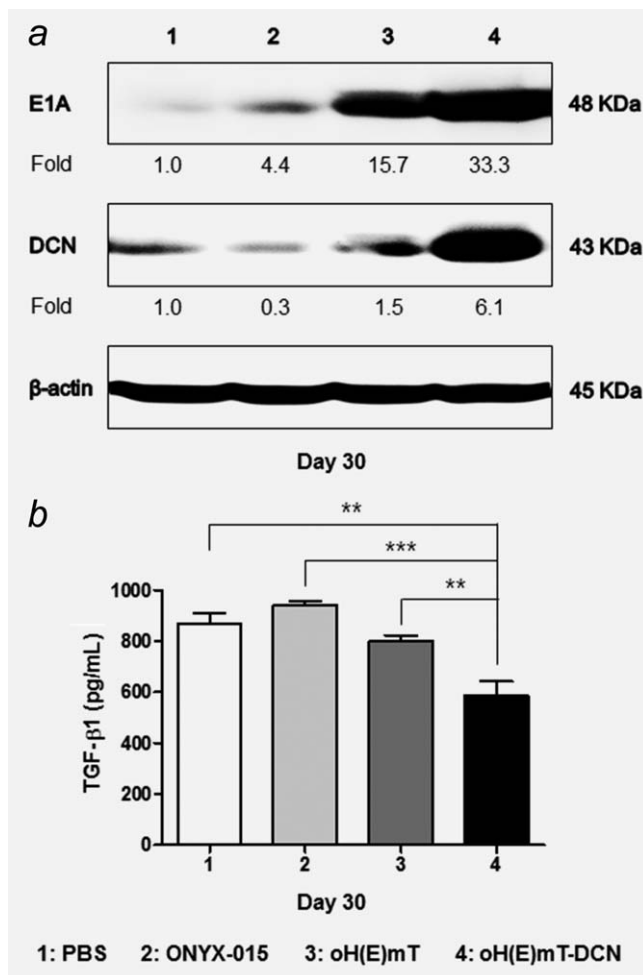


Figure 5. Functional analysis of pancreatic tumor tissue treated with PBS, ONYX-015, oH(E)mT or oH(E)mT-DCN. Western blotting (a) and TGF-β1 ELISA (b) were performed using the resultant tumor lysates. (c) H & E staining, Ad E1A immunohistochemical staining, PCNA immunohistochemical staining and TUNEL assay results from pancreatic cancer tissue. Original magnification: $\times 100$ and $\times 400$. (d) Tumor sections were stained with anti-Ad E1A Abs to examine viral replication (red). HIF-1 α Abs were used to visualize hypoxic regions (green). Normoxic and hypoxic regions are both visible. (e) Masson's trichrome and picrosirius red staining of pancreatic cancer tissue. Collagen expression was analyzed semiquantitatively from the resultant images. Original magnification: $\times 100$ and $\times 400$. (f) Reduced protein levels of ECM components including collagen type I and III, elastin and fibronectin were observed in pancreatic cancer tissue treated with oH(E)mT-DCN compared with tissues treated with the other Ads. Semiquantitative image analysis was performed to measure the protein levels of type I and III collagen, elastin and fibronectin. Significantly reduced levels of type I collagen, type III collagen, elastin and fibronectin were observed in pancreatic cancer tissue treated with oH(E)mT-DCN than in the tumor tissues treated with the control viruses. Original magnification: $\times 400$. The tumor (T) and normal (N) tissues are separated with a dotted line in the oH(E)mT-DCN-treated group. Data are presented as mean \pm SD. * $p < 0.05$, ** $p < 0.01$ and *** $p < 0.001$. [Color figure can be viewed at wileyonlinelibrary.com]

replication were observed in hypoxic tumor regions, whereas no detectable accumulation of ONYX-015 was observed. The levels of oH(E)mT and oH(E)mT-DCN VP in hypoxic tumor

regions were similar to those observed in normoxic regions. This finding demonstrates that the HREs upstream of the cancer-specific promoter can be transactivated by HIF-1 α , which is overexpressed under hypoxia, to overcome hypoxia-mediated downregulation of Ad E1A expression. Importantly, oH(E)mT-DCN was distributed over a larger area and more virus was observed under hypoxic conditions compared with oH(E)mT, indicating that DCN-mediated apoptosis facilitates viral dispersion throughout desmoplastic pancreatic tumors.

DCN has been shown to inhibit TGF- β activity, which plays a critical role in aberrant ECM deposition and the subsequent acquisition of resistance toward therapeutics in pancreatic tumors. Thus, we next assessed the effect of DCN-expressing oncolytic Ad on the ECM in orthotopic pancreatic tumors *via* histological and immunohistochemical staining. Masson's trichrome and picrosirius red staining of pancreatic tumor sections revealed that collagen deposition was significantly decreased in oH(E)mT-DCN-treated tumors compared with ONYX-015-treated or oH(E)mT-treated tumors. As shown in Figure 5e, tumors treated with oH(E)mT-DCN contained less collagen compared with those treated with PBS, ONYX-015, or oH(E)mT (** $p < 0.01$, *** $p < 0.001$). Furthermore, oH(E)mT-DCN-treated tumors exhibited significantly attenuated accumulation of major ECM components such as type I collagen, type III collagen, elastin and fibronectin compared with those treated with PBS, ONYX-015 or oH(E)mT. This finding indicates that oncolytic Ad-mediated expression of DCN effectively degrades overexpressed ECM components in pancreatic tumors (Fig. 5f; * $p < 0.05$, ** $p < 0.01$ or *** $p < 0.001$). Similar results were observed in patient-derived pancreatic tumor spheroids where oH(E)mT-DCN treatment led to degradation of tumor ECM and tumor cell death (Supporting Information Fig. S5). Taken together, these results indicate that oH(E)mT-DCN can efficiently degrade ECM, overcome hypoxia-mediated downregulation of Ad E1A expression, and exhibit potent antitumor efficacy against highly desmoplastic pancreatic tumors.

Therapeutic efficacy of oH(E)mT-DCN in patient-derived pancreatic cancer organoid cultures

Although orthotopic tumor models closely emulate tissue-specific disease progression of clinical tumors, orthotopic implantation in immunodeficient mice does not completely recapitulate tumorigenesis in humans because the tumor microenvironments are not equivalent.³⁰ In this regard, 3D organoid culture of patient tumors, an approach that mimics the ECM components and complex cell heterogeneity of clinical tumors, is a promising model for the evaluation of novel therapeutics.^{31–34} To take advantage of this model system, pancreatic tumor spheroids derived from patient samples were cultured and treated with PBS, ONYX-015, oH(E)mT or oH(E)mT-DCN for 6 days. As shown in Figure 6a and Supporting Information Fig. S5, PBS-treated patient-derived pancreatic tumor spheroids were primarily composed of a

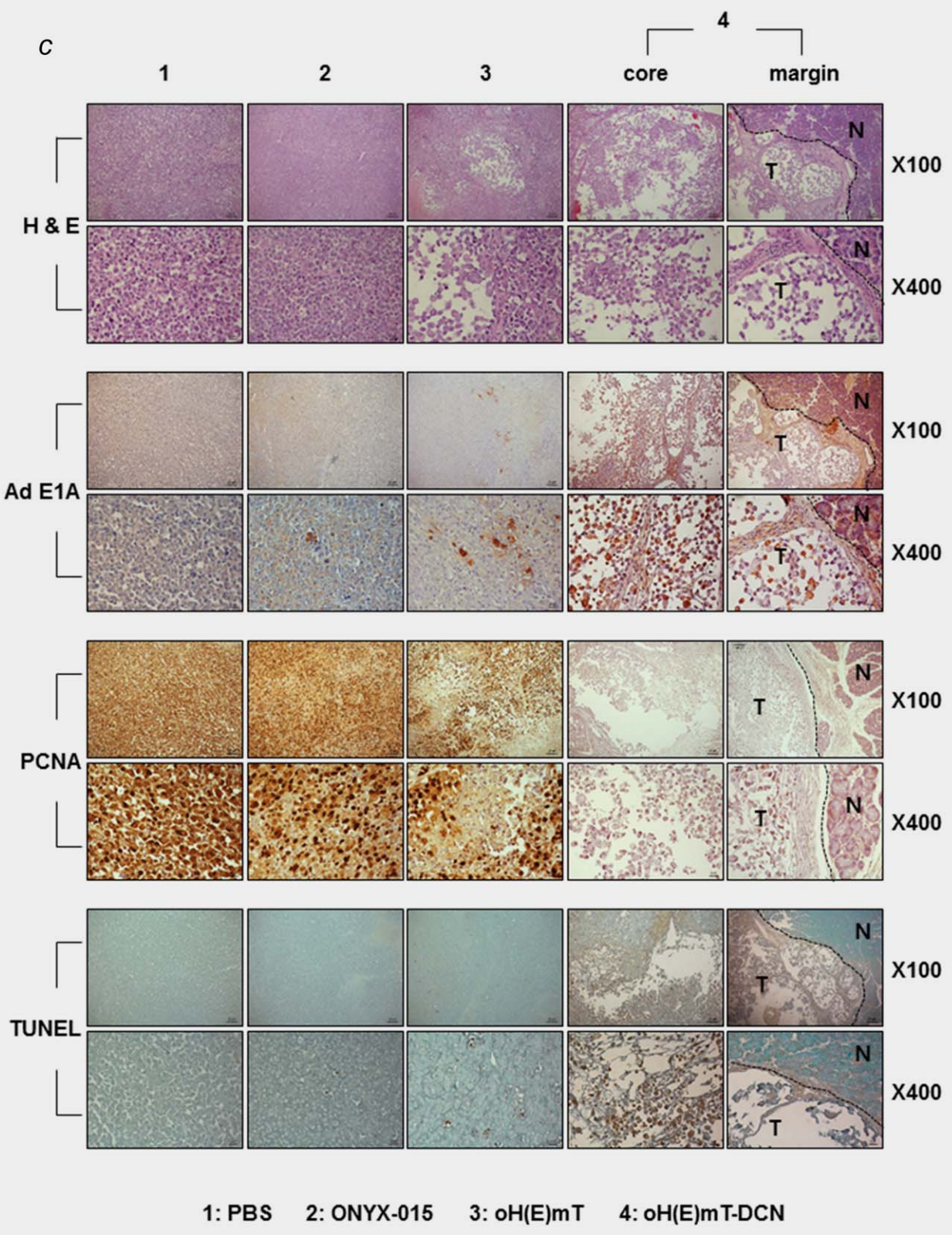


Figure 5. Continued.

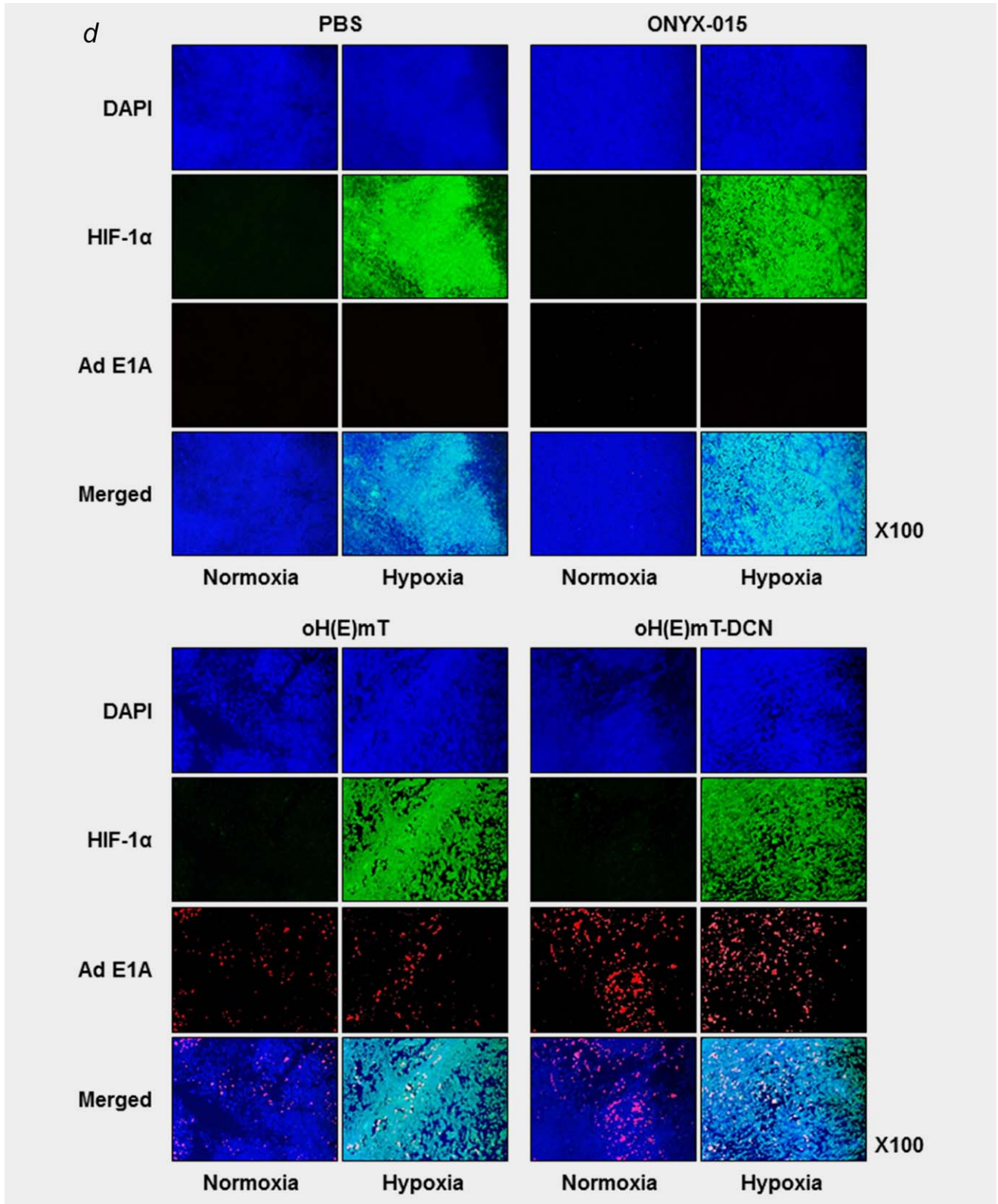


Figure 5. Continued

thick and dense layer of ECM components, similar to orthotopic pancreatic tumors (Fig. 5e). This finding indicates that 3D tumor spheroids and orthotopic models both closely

emulate the desmoplastic attributes of clinical pancreatic tumors. In good agreement with our results from the orthotopic pancreatic tumor model, oH(E)mT-DCN induced

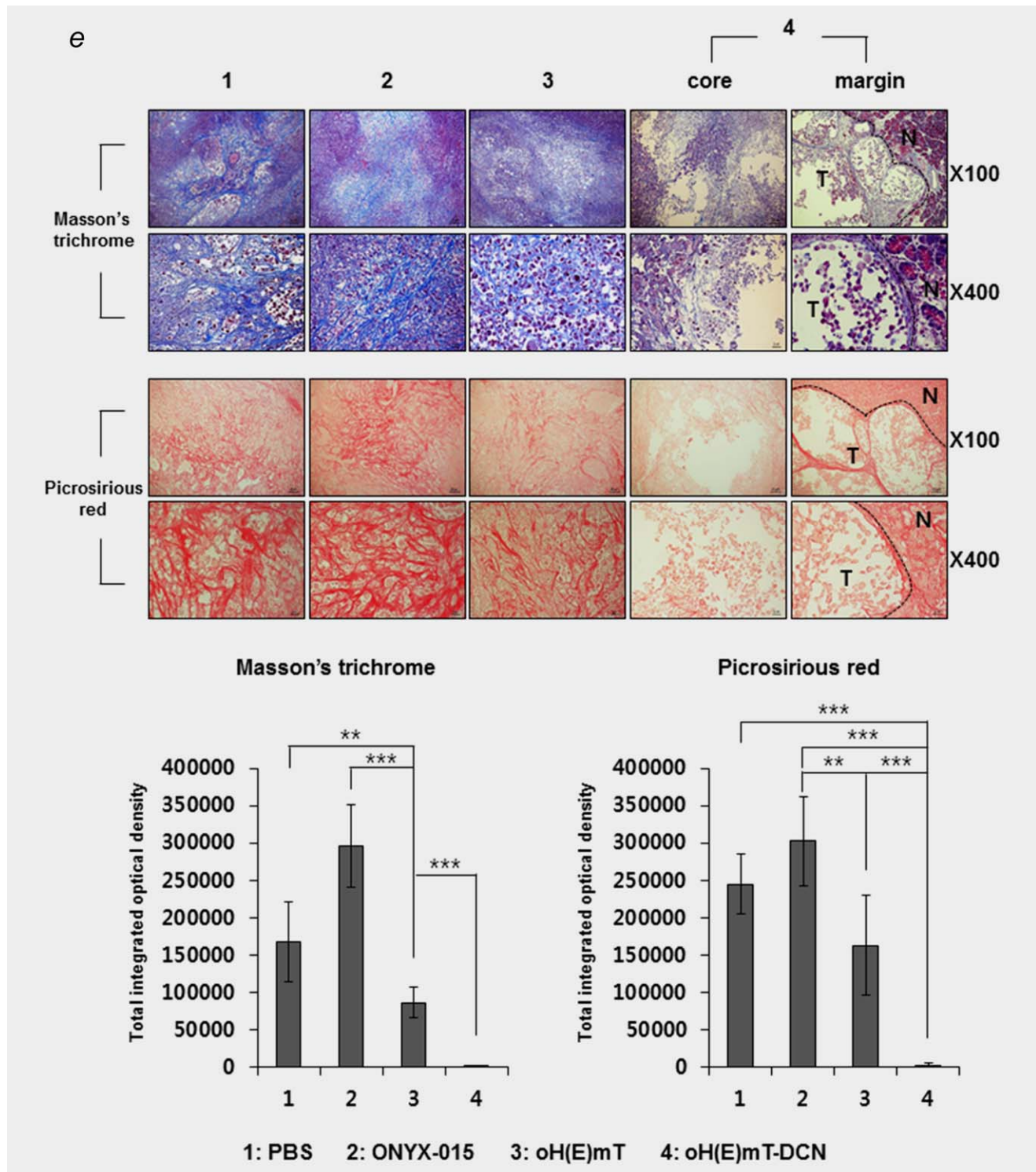


Figure 5. Continued

efficient degradation of major ECM components, attenuated proliferation of tumor cells, induced apoptosis in tumor cells and exhibited proficient viral dissemination in patient-derived tumor spheroids (Figs. 6ac). Together, these results suggest that oH(E)mT-DCN induces potent antitumor effects

by overcoming hypoxia-mediated downregulation of Ad E1A expression and desmoplasia in patient-derived tumor spheroids, suggesting oH(E)mT-DCN as a promising candidate for future clinical trials targeting aggressive and desmoplastic pancreatic cancer.

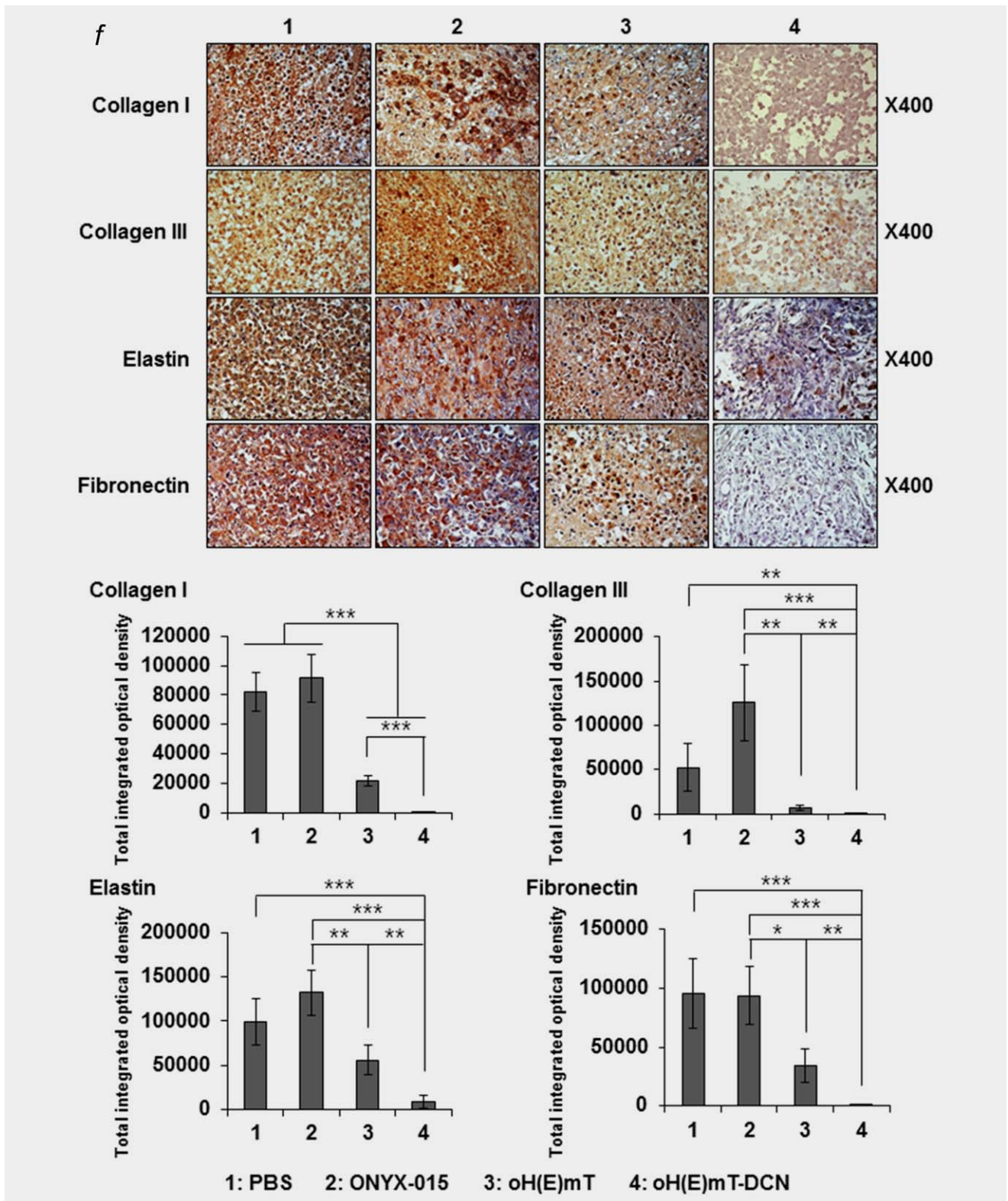


Figure 5. Continued

Discussion

Pancreatic cancer is associated with the worst prognosis of all gastrointestinal malignancies.³⁵⁻³⁷ The major reasons for

these poor outcomes are late diagnosis and poor therapeutic efficacy of conventional treatments, which are due to the nonspecific symptoms and aggressive tumor biology,

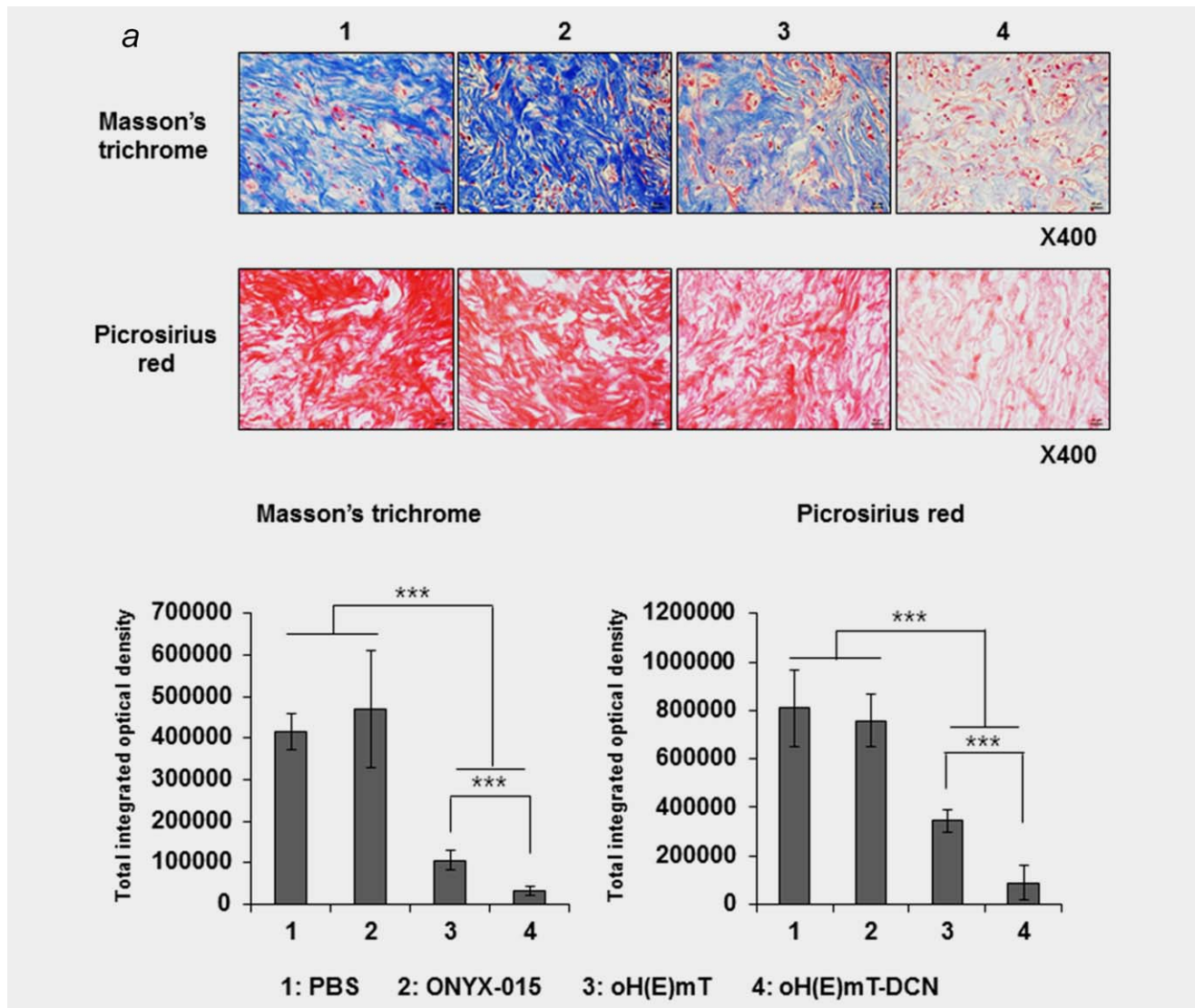


Figure 6. Histological and immunohistochemical staining of pancreatic cancer patient-derived tumor spheroids for type I and III collagen, elastin and fibronectin. (a) Masson's trichrome and Picrosirius red staining of primary pancreatic tumor spheroids treated with PBS, ONYX-015, oH(E)mT or oH(E)mT-DCN. Collagen expression was analyzed semiquantitatively. Original magnification: $\times 400$. (b) Reduced protein levels of various ECM components including collagen type I and III, elastin and fibronectin were observed in primary pancreatic tumor spheroids treated with oH(E)mT-DCN compared with spheroids treated with the other Ads. Type I and III collagen, elastin and fibronectin protein levels were analyzed semiquantitatively. Significantly reduced levels of type I collagen, type III collagen, elastin and fibronectin were observed in primary pancreatic tumor spheroids treated with oH(E)mT-DCN compared with spheroids treated with control viruses. Original magnification: $\times 400$. (c) H & E staining, Ad E1A immunohistochemical staining, PCNA immunohistochemical staining and TUNEL assay results from primary pancreatic tumor spheroids. Original magnification: $\times 400$. PCNA expression and TUNEL assay images were analyzed semiquantitatively. Bars represent mean \pm SD. * $p < 0.05$, ** $p < 0.01$ and *** $p < 0.001$. [Color figure can be viewed at wileyonlinelibrary.com]

respectively. Histologically, pancreatic cancer tumors are extremely stroma-rich and hypovascular. Indeed, most of the pancreatic tumor mass consists of ECM components, such as collagen, desmin, fibronectin and hyaluronic acid.^{38–40} Aberrant accumulation of ECM in the tumor microenvironment is a major obstacle hindering the success of conventional treatments against pancreatic cancer. Gemcitabine, a standard chemotherapeutic prescribed for the treatment of pancreatic cancer, can only prolong life expectancy by 6 months. The

inefficiency of this therapeutic has been shown to be due to poor drug permeation into ECM-rich tumors.^{25,41}

Another critical hurdle for the effective treatment of pancreatic cancer is hypoxia, which refers to the low partial pressure of oxygen and subsequent acidosis that frequently occur in the tumor microenvironment.⁴² HIF-1 α , a potent regulator of the homeostatic transcriptional response to hypoxia, is significantly overexpressed in pancreatic cancer.^{43,44} Importantly, HIF-1 α stimulates transcription of genes that contain

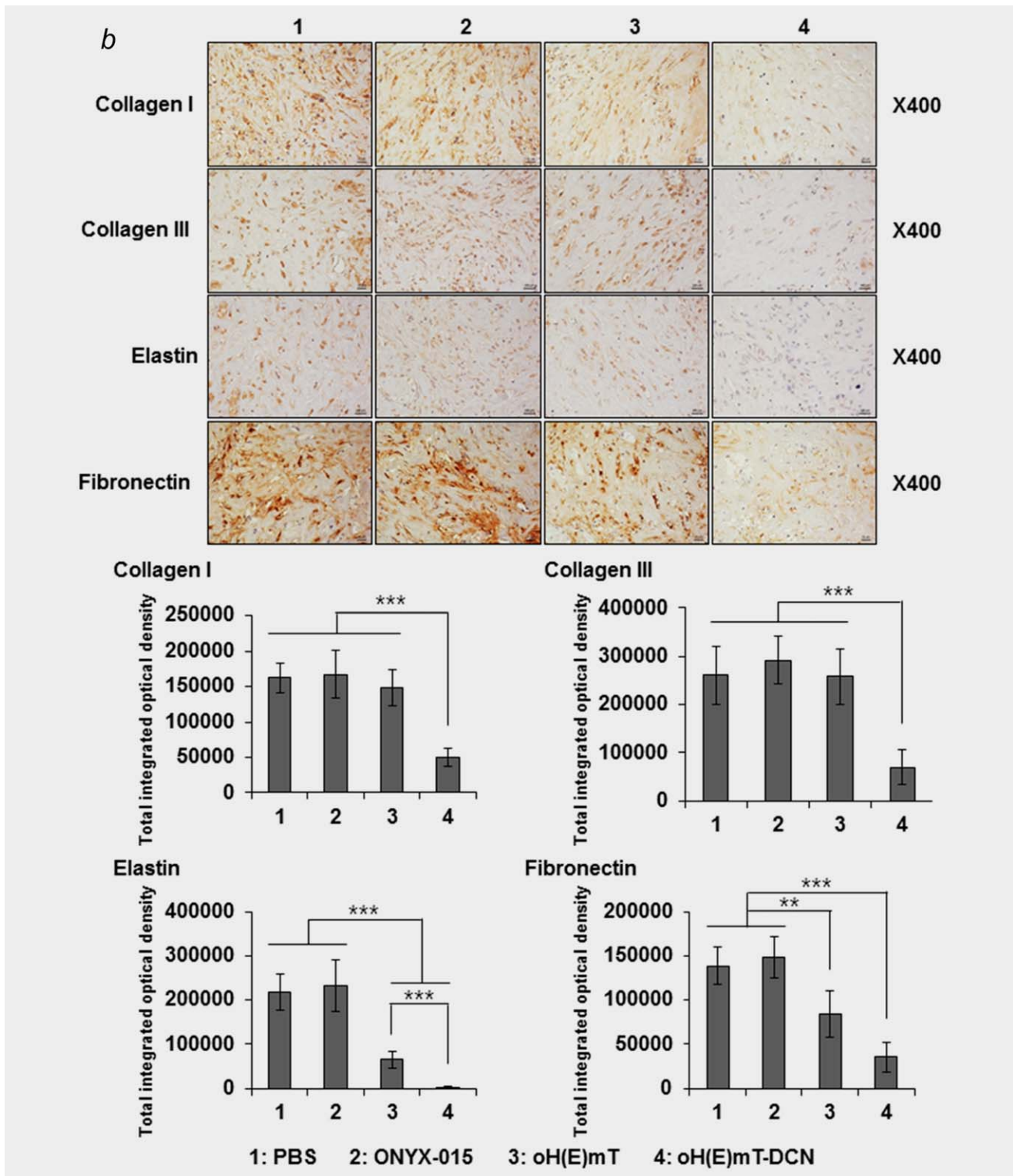


Figure 6. Continued.

HREs in their promoters. Therefore, transcriptional regulation *via* a hypoxia-inducible promoter is frequently employed to target the hypoxic tumor microenvironment.

In this report, we generated two variants of HRE-harboring, cancer-selective hybrid promoters (H(E)mT and

H(mT)E). The levels of transgene expression driven by the H(E)mT promoter and by the H(mT)E promoter were both significantly enhanced under hypoxic conditions, indicating that the HRE enhancer enhances promoter activity under hypoxic conditions. Importantly, the H(E)mT promoter

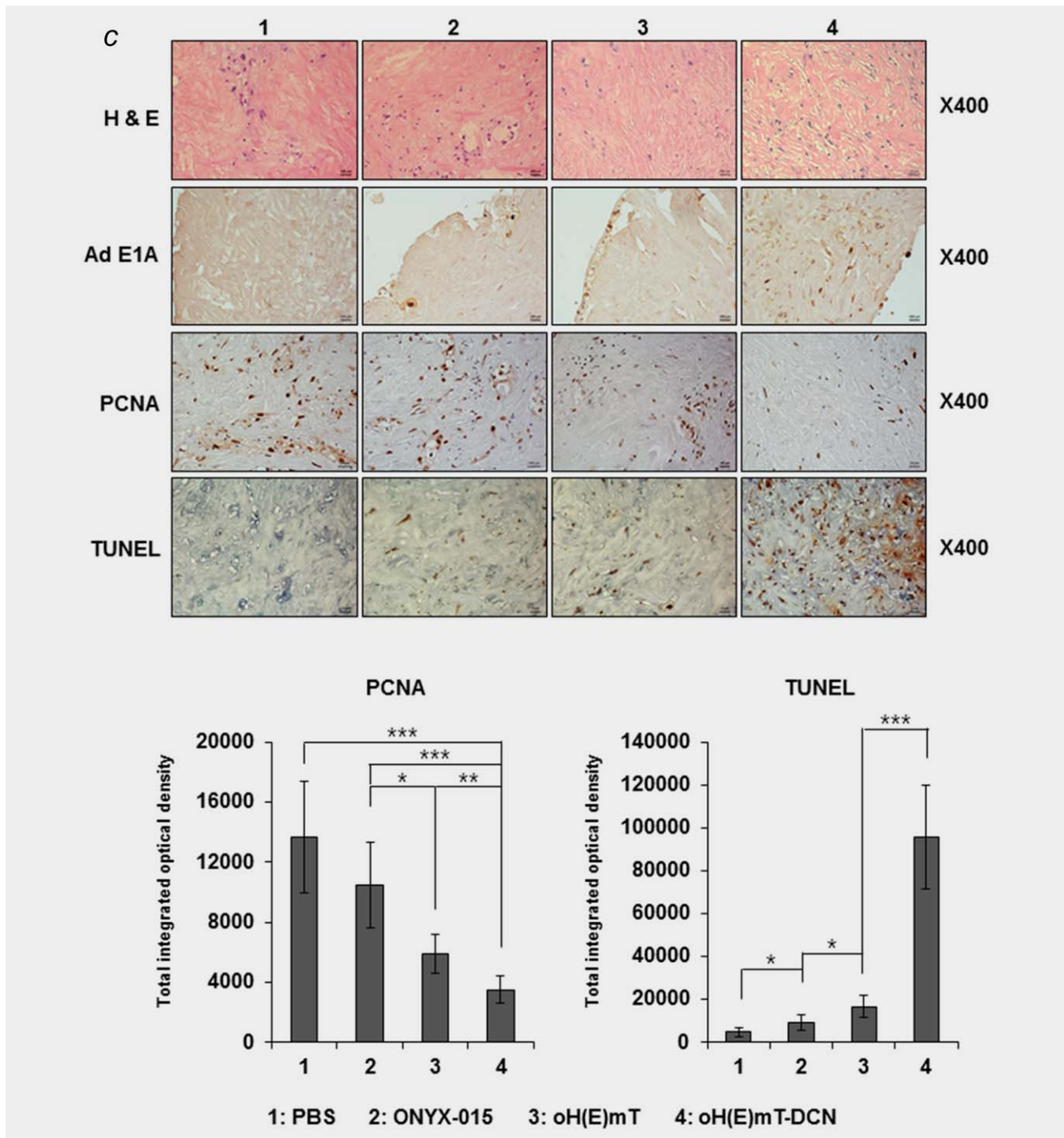


Figure 6. Continued.

induced higher Ad transgene expression than the H(mT)E promoter under both normoxic and hypoxic conditions, demonstrating that the level of transcriptional activity of a given hybrid promoter is affected by the order in which the promoter components are inserted into the Ad genome (Figs. 1a and 1b, Supporting Information Fig. S2A). Since the H(E)mT promoter demonstrated superior promoter activity to that of the H(mT)E promoter, we chose to extensively

characterize the therapeutic efficacy of H(E)mT-harboring Ads. In addition to exhibiting enhanced transcription in hypoxic conditions, H(E)mT-driven expression of GFP was highly cancer-specific. This finding indicates that our novel H(E)mT hybrid promoter is a good candidate for regulating Ad E1A gene expression of oncolytic Ad in a manner that endows cancer specificity (Figs. 1c and 1d, Supporting Information Fig. S2B). Oncolytic Ad replicating under the control

of the H(E)mT promoter (oH(E)mT) was highly cytotoxic to cancer cells and exhibited significant replication in a highly cancer-specific manner under both normoxic and hypoxic conditions (Figs. 2 and 3). These findings are in good agreement with our previous report, in which we demonstrated the cancer selectivity of HRE-mediated enhancement of oncolytic Ad transgene expression under hypoxic conditions.¹⁰ Of note, oH(E)mT exhibited greater viral replication than oRd19, a control oncolytic Ad with the endogenous Ad promoter, in cancer cells. In contrast, no evident cytotoxicity was observed in normal cells, implying that the potent and cancer-specific killing effect of oH(E)mT is mediated by efficient and preferential replication of oncolytic Ad in cancer cells (Figs. 2 and 3).

Current trends of oncolytic Ad development for clinical applications have focused on armed oncolytic Ads expressing anticancer therapeutic genes. Several clinical studies have evaluated the efficacy of these Ads against various types of cancers.^{45–47} In the context of this strategy, we generated oncolytic Ad expressing DCN, a potent inducer of tumor cell apoptosis and ECM degradation, as a potential candidate for the treatment of desmoplastic pancreatic cancer. DCN-expressing oncolytic Ad (oH(E)mT-DCN) induced a dose-dependent increase in DCN expression in a cancer cell-specific manner (Fig. 3a). Furthermore, oH(E)mT-DCN exhibited dose-dependent cytotoxicity in a cancer cell-specific manner that was superior to that of its cognate control oncolytic Ad oH(E)mT, indicating that the dose-dependent increase in DCN achieved with oH(E)mT-DCN was responsible for the enhanced anticancer effect (Fig. 3b). Moreover, oH(E)mT-DCN was more highly cytotoxic than oH(E)mT, in a time-dependent manner, further demonstrating that amplification of DCN and oncolytic Ad *via* active viral replication resulted in potent cancer cell killing (Fig. 3b). Of particular interest, only negligible oH(E)mT-DCN-induced DCN expression was detected in normal cells, and no cytotoxicity was observed, findings that are in good agreement with a previous report demonstrating that DCN-induced apoptosis was cancer-specific.⁴⁸ Similar results were observed *in vivo*; that is, oH(E)mT-DCN exhibited superior antitumor efficacy *via* DCN-mediated induction of apoptosis and active viral replication within highly aggressive and desmoplastic orthotopic pancreatic tumor tissue compared to its cognate control oH(E)mT (Figs. 4a–4c and 5a). Furthermore, normal tissue adjacent to the tumor was not affected by oH(E)mT-DCN. These findings are in good agreement with previous reports demonstrating that DCN induces cancer-selective apoptosis but is not detrimental to normal cells, providing further support for the idea that low level expression level of Ad-mediated DCN in normal cells is not harmful.^{14,26}

The ECM is a critical hurdle complicating oncolytic Ad-mediated gene therapy for the treatment of pancreatic cancer, since the coarse and dense ECM prevents penetration and dispersion of Ad into tumor tissue. TGF- β is a key profibrotic cytokine that induces ECM accumulation in pancreatic

tumors by inhibiting proteolytic enzymes. DCN harbors a high-affinity binding site for TGF- β ; thus, binding of DCN to TGF- β neutralizes its biological activity.¹³ We found that TGF- β protein level was significantly reduced by oH(E)mT-DCN in orthotopic pancreatic tumor tissue, supporting the idea that DCN is a natural inhibitor of TGF- β (Fig. 5b). Importantly, DCN-mediated suppression of TGF- β following oH(E)mT-DCN treatment was positively correlated with attenuation in the expression levels of major ECM components, such as collagen types I & III, fibronectin and elastin, indicating that oncolytic Ad-mediated expression of DCN can effectively degrade ECM components in tumor tissue *via* downregulation of the profibrotic cytokine TGF- β (Figs. 5a–5e and 5f). These results are in good agreement with previous reports by our group and others demonstrating that DCN delays the lateral assembly of collagen fibrils⁴⁹ and downregulates the production of other ECM components by blocking the activity of TGF- β ,^{49,50} ultimately resulting in enhanced dispersion of oncolytic virus in tumor tissues through degradation of tumor ECM.¹⁴ In addition, the DCN expression level and extent of ECM component degradation were both positively correlated with Ad dispersion and accumulation within pancreatic tumors. These findings are in good agreement with a previous report, demonstrating that DCN enhances Ad penetration and distribution within solid tumors *via* ECM degradation.¹⁴ Alternatively, induction of apoptosis has been reported to enhance viral dispersion within solid tumors by transferring Ad progeny virus to neighboring tumor cells *via* apoptotic bodies and attenuating intratumoral interstitial pressure.⁵¹ In good agreement with this report, oH(E)mT-DCN potently induced apoptosis in tumor tissue; furthermore, this effect was positively correlated with the extent of viral dispersion and replication within solid tumors. Together, these results demonstrate that oH(E)mT-DCN potently induces apoptosis and efficient degradation of ECM components, thereby resulting in high levels of viral dissemination and active replication within orthotopic pancreatic tumor tissue.

Hypovascularization within solid tumors has been demonstrated to suppress replication of oncolytic Ad, resulting in poor and uneven viral distribution in tumor tissue.^{11,12} The HRE enhancer, which binds to overexpressed HIF-1 α under hypoxic conditions and induces transactivation of its downstream promoters, has been frequently employed to achieve tumor selectivity. Oncolytic Ad replicating under the control of our novel HRE-harboring cancer-specific hybrid promoter H(E)mT (oH(E)mT) showed enhanced viral replication under hypoxic conditions compared with normoxic conditions. Thus, our strategy was able to overcome hypoxia-induced downregulation of Ad E1A expression both *in vitro* and *in vivo* (Figs. 2b, 2c and 5d). Furthermore, the level of Ad E1A expression achieved with oH(E)mT-DCN was markedly higher than that achieved with ONYX-015 or its cognate control, oH(E)mT, in hypoxic tumor regions. Together, these results demonstrate that the combination of a hypoxia-

responsive promoter with intratumoral expression of DCN can yield enhanced viral replication and dispersion of oH(E)mT-DCN in hypovascular tumor regions, as well as in normoxic regions of ECM-rich pancreatic tumors.

3D organoid culture of primary patient tumors can provide a more accurate representation of the clinical tumor microenvironment compared with orthotopic xenograft models. Furthermore, 3D patient tumor spheroids retain their heterogeneous tumor cell populations as well as the complex network of cell-cell and cell-matrix interactions exhibited in clinical tumors, making this model a promising candidate for evaluating the penetration and action of novel therapeutics.^{52,53} In this study, both orthotopic pancreatic tumors and tumor spheroids derived from patients with pancreatic cancer exhibited aberrantly high deposition of ECM components. These characteristics closely emulate the desmoplastic attributes of clinical pancreatic cancer described in previous literature (Figs. 5e and 6a). In both orthotopic tumors and

primary patient spheroids, oH(E)mT-DCN effectively induced tumor cell apoptosis, ECM degradation and dispersion of Ad in both normoxic and hypoxic tumor regions, leading to a potent tumoricidal effect.

In summary, we demonstrated that a novel DCN-expressing oncolytic Ad, oH(E)mT-DCN, can potently inhibit tumor growth through a multifunctional process. In this process, degradation of ECM, hypoxia responsiveness and induction of apoptosis facilitate dispersion and active replication of oncolytic Ad in both normoxic and hypoxic regions of desmoplastic pancreatic tumors that closely emulate clinical tumors. These findings suggest oH(E)mT-DCN as a promising therapeutic candidate for future clinical trials against aggressive pancreatic cancer.

Acknowledgement

All authors had input into the manuscript and have approved the manuscript for publication.

References

- Malvezzi M, Bertuccio P, Levi F, et al. European cancer mortality predictions for the year 2014. *Ann Oncol* 2014;25:1650–6.
- Siegel R, Naishadham D, Jemal A. Cancer statistics, 2013. *CA Cancer J Clin* 2013;63:11–30.
- Laheru D, Biedrzycki B, Jaffee EM. Development of a cytokine-modified allogeneic whole cell pancreatic cancer vaccine. *Methods Mol Biol* 2013; 175–203.
- Eager R, Nemunaitis J. Clinical development directions in oncolytic viral therapy. *Cancer Gene Ther* 2011;18:305–17.
- Sinkovics J, Horvath J. New developments in the virus therapy of cancer: a historical review. *Intervirology* 1993;36:193–214.
- Toth K, Dhar D, Wold WS. Oncolytic (replication-competent) adenoviruses as anticancer agents. *Expert Opin Biol Ther* 2010;10:353–68.
- Xia ZJ, Chang JH, Zhang L, et al. Phase III randomized clinical trial of intratumoral injection of E1B gene-deleted adenovirus (H101) combined with cisplatin-based chemotherapy in treating squamous cell cancer of head and neck or esophagus. *Ai Zheng* 2004;23:1666–70.
- FAC. RHIA. A randomized phase III trial of talimogene laherparepvec (T-VEC) versus subcutaneous (SC) granulocyte-macrophage colony-stimulating factor (GM-CSF) for the treatment (tx) of unresected stage IIIB/C and IV melanoma. *J Clin Oncol* 2013;31(suppl;abstract LBA9008).
- Erickson LA, Highsmith WE, Jr., Fei P, et al. Targeting the hypoxia pathway to treat pancreatic cancer. *Drug Des Devel Ther* 2015;9:2029–31.
- Kwon OJ, Kim PH, Huyn S, et al. A hypoxia- and {alpha}-fetoprotein-dependent oncolytic adenovirus exhibits specific killing of hepatocellular carcinomas. *Clin Cancer Res* 2010;16: 6071–82.
- Shen BH, Hermiston TW. Effect of hypoxia on Ad5 infection, transgene expression and replication. *Gene Ther* 2005;12:902–10.
- Pipiya T, Sauthoff H, Huang YQ, et al. Hypoxia reduces adenoviral replication in cancer cells by downregulation of viral protein expression. *Gene Ther* 2005;12:911–7.
- Yamaguchi Y, Mann DM, Ruoslahti E. Negative regulation of transforming growth factor-beta by the proteoglycan decorin. *Nature* 1990;346:281–4.
- Choi IK, Lee YS, Yoo JY, et al. Effect of decorin on overcoming the extracellular matrix barrier for oncolytic virotherapy. *Gene Ther* 2010;17:190–201.
- Hemminki O, Parviainen S, Juhila J, et al. Immunological data from cancer patients treated with Ad5/3-E2F-Delta24-GMCSF suggests utility for tumor immunotherapy. *Oncotarget* 2015;6:4467–81.
- Lanson NA, Jr., Friedlander PL, Schwarzenberger P, et al. Replication of an adenoviral vector controlled by the human telomerase reverse transcriptase promoter causes tumor-selective tumor lysis. *Cancer Res* 2003;63:7936–41.
- Kim E, Kim JH, Shin HY, et al. AdmTERTD19, a Conditional Replication Competent Adenovirus Driven by the Human Telomerase Promoter, Selectively Replicates in and Elicits Cytopathic Effect in a Cancer Cell-Specific Manner. *Hum Gene Ther* 2003;14:1415–1428.
- Hemminki O, Parviainen S, Juhila J, Turkki R, Linder N, Lundin J, Kankainen M, Ristimäki A, Koski A, Liikanen I. Immunological data from cancer patients treated with Ad5/3-E2F-Δ24-GMCSF suggests utility for tumor immunotherapy. *Oncotarget*. 2015;6:4467.
- Lee JS, Hur MW, Lee SK, et al. A novel sLRP6E1E2 inhibits canonical Wnt signaling, epithelial-to-mesenchymal transition, and induces mitochondria-dependent apoptosis in lung cancer. *PLoS One* 2012;7:e36520
- Kim EK, Seo HS, Chae MJ, et al. Enhanced antitumor immunotherapeutic effect of B-cell-based vaccine transduced with modified adenoviral vector containing type 35 fiber structures. *Gene Ther* 2014;21:106–14.
- Kim J, Kim JH, Choi KJ, et al. E1A- and E1B-Double mutant replicating adenovirus elicits enhanced oncolytic and antitumor effects. *Hum Gene Ther* 2007;18:773–86.
- Yoon AR, Kim JH, Lee YS, et al. Markedly enhanced cytotoxicity by E1B-19kD-deleted oncolytic adenovirus in combination with cisplatin. *Hum Gene Ther* 2006;17:379–90.
- Yun CO, Kim E, Koo T, et al. ADP-overexpressing adenovirus elicits enhanced cytopathic effect by induction of apoptosis. *Cancer Gene Ther* 2005;12:61–71.
- Kim J, Cho JY, Kim JH, et al. Evaluation of E1B gene-attenuated replicating adenoviruses for cancer gene therapy. *Cancer Gene Ther* 2002;9:725–36.
- Whatcott CJ, Posner RG, Von Hoff DD, et al. Desmoplasia and chemoresistance in pancreatic cancer In: Grippo PJ, Munshi HG, eds. Pancreatic Cancer and Tumor Microenvironment. Trivandrum, India: Transworld Research Network, 2012.
- Na Y, Choi JW, Kasala D, et al. Potent antitumor effect of neurotensin receptor-targeted oncolytic adenovirus co-expressing decorin and Wnt antagonist in an orthotopic pancreatic tumor model. *J Control Release* 2015;220:766–82.
- Weber HL, Gidekel M, Werbach S, et al. A Novel CDC25B Promoter-Based Oncolytic Adenovirus Inhibited Growth of Orthotopic Human Pancreatic Tumors in Different Preclinical Models. *Clin Cancer Res* 2015;21:1665–74.
- Pickup M, Novitskiy S, Moses HL. The roles of TGFbeta in the tumour microenvironment. *Nat Rev Cancer* 2013;13:788–99.
- Lee WJ, Ahn HM, Roh H, et al. Decorin-expressing adenovirus decreases collagen synthesis and upregulates MMP expression in keloid fibroblasts and keloid spheroids. *Exp Dermatol* 2015;24:591–7.
- Qiu W, Su GH. Development of orthotopic pancreatic tumor mouse models. *Methods Mol Biol* 2013;980:215–23.
- Hwang CI, Boj SF, Clevers H, et al. Preclinical models of pancreatic ductal adenocarcinoma. *J Pathol* 2016;238:197–204.
- Boj SF, Hwang CI, Baker LA, et al. Organoid models of human and mouse ductal pancreatic cancer. *Cell* 2015;160:324–38.
- Whittle JR, Lewis MT, Lindeman GJ, et al. Patient-derived xenograft models of breast cancer and their predictive power. *Breast Cancer Res* 2015;17: 17.

34. Malaney P, Nicosia SV, Dave V. One mouse, one patient paradigm: new avatars of personalized cancer therapy. *Cancer Lett* 2014;344:1–12.
35. Singh HM, Ungerechts G, Tsimberidou AM. Gene and cell therapy for pancreatic cancer. *Expert Opin Biol Ther* 2015;15:505–16.
36. Siegel R, Naishadham D, Jemal A. Cancer statistics, 2013. *CA Cancer J Clin* 2013;63:11–30.
37. Yadav D, Lowenfels AB. The epidemiology of pancreatitis and pancreatic cancer. *Gastroenterology*. 2013;144:1252–61.
38. Erkan M, Hausmann S, Michalski CW, et al. The role of stroma in pancreatic cancer: diagnostic and therapeutic implications. *Nat Rev Gastroenterol Hepatol* 2012;9:454–67.
39. Neesse A, Michl P, Frese KK, et al. Stromal biology and therapy in pancreatic cancer. *Gut* 2011;60:861–8.
40. Wormann SM, Diakopoulos KN, Lesina M, et al. The immune network in pancreatic cancer development and progression. *Oncogene* 2014;33:2956–67.
41. Ying JE, Zhu LM, Liu BX. Developments in metastatic pancreatic cancer: is gemcitabine still the standard? *World J Gastroenterol* 2012;18:736–45.
42. Vaupel P, Thews O, Hoeckel M. Treatment resistance of solid tumors: role of hypoxia and anemia. *Med Oncol* 2001;18:243–59.
43. Koong AC, Mehta VK, Le QT, et al. Pancreatic tumors show high levels of hypoxia. *Int J Radiat Oncol Biol Phys* 2000;48:919–22.
44. Ye LY, Zhang Q, Bai XL, et al. Hypoxia-inducible factor 1alpha expression and its clinical significance in pancreatic cancer: a meta-analysis. *Pancreatol* 2014;14:391–7.
45. Yoon A, W Kim S, Yun C-O. Armed oncolytic adenoviruses and polymer-shielded nanocomplex for systemic delivery. *Curr Cancer Ther Rev* 2015;11:136–53.
46. Bramante S, Koski A, Liikanen I, et al. Oncolytic virotherapy for treatment of breast cancer, including triple-negative breast cancer. *Oncoimmunology* 2016;5:e1078057
47. Kanerva A, Nokisalmi P, Diaconu I, et al. Antiviral and antitumor T-cell immunity in patients treated with GM-CSF-coding oncolytic adenovirus. *Clin Cancer Res* 2013;19:2734–44.
48. Tralhao JG, Schaefer L, Micegova M, et al. In vivo selective and distant killing of cancer cells using adenovirus-mediated decorin gene transfer. *FASEB J* 2003;17:464–6.
49. Goldoni S, Iozzo RV. Tumor microenvironment: Modulation by decorin and related molecules harboring leucine-rich tandem motifs. *Int J Cancer* 2008;123:2473–9.
50. Cabello-Verrugio C, Brandan E. A novel modulatory mechanism of transforming growth factor-beta signaling through decorin and LRP-1. *J Biol Chem* 2007;282:18842–50.
51. Mi J, Li ZY, Ni S, et al. Induced apoptosis supports spread of adenovirus vectors in tumors. *Hum Gene Ther* 2001;12:1343–52.
52. Longati P, Jia X, Eimer J, et al. 3D pancreatic carcinoma spheroids induce a matrix-rich, chemoresistant phenotype offering a better model for drug testing. *BMC Cancer* 2013;13:95.
53. Kim JB. Three-dimensional tissue culture models in cancer biology. *Semin Cancer Biol* 2005;15:365–77.